CSIAM Trans. Life Sci.
doi: 10.4208/csiam-ls.SO-2025-0024

Vol. **x**, No. x, pp. 1-42
xx 2025

Vegetation Patterns: Structures and Dynamics

Li-Feng Hou[1,2,3], Jun Zhang[4,5], Gui-Quan Sun[1,2,3,*] and Zhen Jin[2,3,*]

[1] *School of Mathematics, North University of China, Taiyuan 030051, China.*
[2] *Complex Systems Research Center, Shanxi University, Taiyuan 030006, China.*
[3] *Key Laboratory of Complex Systems and Data Science of Ministry of Education, Taiyuan 030006, China.*
[4] *Applied Math Lab, Courant Institute, New York University, New York, NY 10012, USA.*
[5] *New York University-East China Normal University Institute of Physics, New York University Shanghai, Shanghai 200062, China.*

Received 1 August 2025; Accepted 19 October 2025

Abstract. Vegetation patterns are a hallmark of ecosystem self-organization, emerging from the intrinsic dynamics of nonlinear feedback mechanisms and spatiotemporal interactions. This review systematically explores and examines the structural characteristics of these patterns, the phenomena of multistability, and their implications for ecosystem stability through the lens of mathematical modeling and dynamical systems theory. In particular, reaction-diffusion models serve as a key analytical tool, revealing how local positive feedback and non-local negative feedback drive self-organized spatial structures via Turing bifurcation. Bifurcation theory and potential landscape analysis further elucidate ecosystem multistability, quantifying critical transitions among uniform vegetation, patterned states, and bare soil under environmental conditions. Advances in spatial metrics, including traditional statistical measures (e.g. variance, autocorrelation) and emerging complexity-based indicators (e.g. hyperuniformity, spatial permutation entropy) provide robust methods for detecting ecological functional shifts and early-warning signs of regime shifts. Additionally, restoration strategies grounded in structural optimization, such as optimal control theory, offer a theoretical framework for vegetation pattern reconstruction and stability regulation, particularly in arid and semi-arid regions. Future research should integrate multiscale modeling and interdisciplinary approaches to deepen our understanding of vegetation structure-function relationships. Such efforts will yield both theoretical insights and practical solutions for mitigating global ecological degradation and climate change.

AMS subject classifications: 35K57, 35B36, 92C80

Key words: Vegetation patterns, ecosystem stability, multistability, optimal control, critical transitions.

*Corresponding author. *Email addresses:* gquansun@126.com (G.-Q. Sun), jinzhn@263.net (Z. Jin)

1 Introduction

Vegetation patterns are a critical characteristic of ecosystems, serving as the "fingerprints" of ecosystems, containing rich ecological information. These patterns reflect the spatial distribution of vegetation, including uniform, patchy, and striped distribution, which result from complex interactions between biotic and abiotic factors [55,93,114,118]. In arid and semi-arid regions, vegetation commonly forms patchy distributions separated by bare soil or sparsely vegetated areas, reflecting both the scarcity of water resources and adaptive strategies for resource competition. Analyzing vegetation patterns enables the assessment of resource allocation and provides insights into ecosystem health and stability. In addition to serving as indicators of ecosystem states, vegetation patterns play a fundamental role in ecosystem functioning [25, 66, 75, 82, 101, 132]. Different spatial patterns significantly influence nutrient cycling, energy flows, and biodiversity maintenance. Patterns with high connectivity facilitate species migration and dispersal, contributing to population stability. Moreover, well-organized patterns improve resource use efficiency, enhance resilience to disturbances, and strengthen recovery potential. Consequently, the study of vegetation patterns is essential for understanding ecosystem mechanisms, predicting ecological changes, and developing effective strategies for ecological management.

In recent years, significant progress have been made in understanding the mechanisms underlying vegetation pattern formation and advancing theoretical models [13, 34, 76, 86, 102, 104, 119, 131]. Classical nonlinear dynamic models, such as the Klausmeier [55], Rietkerk [41, 84], and Gilad models [35, 36], have been the foundational tools for elucidating the formation and evolution of vegetation patterns. These models describe how positive and negative feedback mechanisms drive pattern formation through the interplay of water dynamics: positive feedback promotes vegetation growth by locally accumulating water, while negative feedback constrains overexpansion via resource competition. In arid and semi-arid regions, these mechanisms lead to the emergence of patchy or striped vegetation patterns, highlighting the critical role of water as a limiting resource. With the advancement of research, these foundational models have been extended to accommodate more complex ecosystem dynamics. For example, introducing time-delay effects can capture the lag in vegetation responses to environmental changes, which is crucial for studying ecosystem dynamics under climate change and human disturbances [46, 109, 123]. Additionally, the influence of plant reproductive strategies (e.g. seed dispersal distances and mechanisms) has been integrated into modeling frameworks [1, 7, 27, 28, 81, 120]. Furthermore, the integration of competitive behaviors among plants, such as root distribution competition for water and nutrients, further refine models to better represent resource allocation and competition processes [59, 69, 80]. Notably, recent research have increasingly focused on coupling vegetation models with climate systems to explore bidirectional effect between vegetation and climate [19, 20, 54, 78, 103]. For instance, changes in precipitation patterns not only influence vegetation distribution but also modify regional climates via evapotran-

spiration, which in turn affects vegetation growth. This coupling mechanism provides a robust theoretical framework for understanding the dynamic evolution of vegetation patterns in the context of climate change, significantly enhancing the predictive ability of these models.

Additionally, the relationship between vegetation patterns and ecosystem stability has garnered increasing attention [15, 29, 65, 99, 100]. Studies on critical transitions in ecosystems suggest that the dynamic characteristics of vegetation patterns can serve as early warning signs for ecosystem degradation [44, 83, 85, 89, 90, 133]. Here, critical transitions refer to the abrupt shifts from one stable state to another, driven by external disturbances or changes in internal conditions [31, 42, 56, 64, 87, 91]. Unlike gradual ecological changes, critical transitions are characterized by nonlinearity, abruptness, and irreversibility, and are signs that the health of the ecosystem has been radically altered. A typical example is the sudden shift of vegetation from a healthy, uniform distribution to a degraded, desertified state [8,10,40,67,85]. A defining feature of critical transitions is the presence of multiple stable states, wherein ecosystems under identical environmental conditions can reside in different configurations. Taking arid and semi-arid regions as an example, under moderate precipitation, vegetation may maintain a healthy distribution, but reduced rainfall or intensified disturbances can push the system into a degraded state [30,77,128,130]. Critical transitions are often accompanied by early warning signals (EWS), exemplified as critical slowing down, characterized by a diminished capacity of a system to recuperate from disturbances as it nears a threshold [12, 14, 91, 117]. This phenomenon is often characterized using spatial metrics, including spatial variance and skewness [16, 23, 24, 38, 39, 88]. Additionally, other morphological changes in vegetation patterns, such as increased patch spacing and irregular shapes, provide critical visual indicators of ecosystem degradation [52, 53, 63, 68, 121]. Together, these statistical metrics and morphological signals enable researchers to detect early indicators of ecological instability, offering critical insights for implementing timely interventions and designing effective restoration strategies.

To reveal the importance of vegetation patterns in ecosystems and their profound relationship with stability, it is necessary to systematically summarize and classify relevant research. Due to the interdisciplinary nature of the subject, vegetation patterns have been approached from many different research angles. Significant progress has been made in understanding vegetation pattern formation, ecosystem stability, and their dynamic evolution, these research results are scattered in different fields, such as nonlinear dynamics, biogeochemical cycling, and ecological management, and lack systematic integration. Moreover, as climate change and human activities increasingly disrupt ecosystems, bridging the gap between theoretical research and practical applications becomes much needed. This review aims to summarize the latest progress in vegetation pattern research, analyze the mechanisms underlying their formation and functional characteristics, and explore their dynamic relationships with ecosystem stability. This review also aims to provide scientific basis and technical support for intervening in ecological degradation and formulating management strategies.

Compared with earlier major reviews on vegetation patterns [52,73,75,86], this paper makes three specific contributions. Firstly, it synthesizes recent progress on multistability and nonlinear dynamics, highlighting their implications for ecosystem resilience. Secondly, it systematically reviews both traditional and emerging indicators of critical transitions, thus linking theoretical insights with practical early-warning applications. Thirdly, it introduces optimal control theory as a new perspective, integrating control-based restoration strategies with classical pattern-formation models. Taken together, these contributions provide a unified framework that bridges fundamental theory with management-oriented applications.

The review is organized as follows. Section 2 introduces the mechanisms of vegetation pattern formation and their links to ecosystem stability, focusing on positive and negative feedbacks, multistability. Section 3 discusses vegetation patterns as indicators of ecosystem resilience, including their role as early warning signals of critical transitions, and further examines restoration and reconstruction strategies based on optimal control theory and related approaches. Section 4 outlines future directions, emphasizing the integration of theoretical models, remote sensing technologies, and artificial intelligence, as well as cross-scale and interdisciplinary perspectives to enhance the application of vegetation pattern research in ecosystem management.

2 Vegetation pattern formation mechanisms and ecosystem stability

Vegetation patterns emerge as spatial manifestations of the complex organism-environment interactions shaped by resource distribution, biological behaviors, and environmental pressures. As a classic example of spatial self-organization, the mechanisms underlying vegetation pattern formation are closely linked to ecosystem stability, and this connection is particularly pronounced in arid and semi-arid ecosystems. The interplay between positive and negative feedback mechanisms could enable the system to maintain stability under varying environmental conditions. Furthermore, the phenomenon of multistability reveals how the system transitions between different stable states. This section will explore the mechanisms of vegetation pattern formation and their relationship with ecosystem stability from two perspectives: positive and negative feedback mechanisms and multistability phenomena.

2.1 Positive and negative feedback mechanisms

Positive and negative feedback mechanisms are the core driving forces behind vegetation pattern formation and maintenance [92]. Mathematical modeling provides a powerful tool to elucidate the role of these mechanisms. By analyzing the dynamics of positive and negative feedback, one can gain deeper insights into the spatial structure, formation conditions, and stability of vegetation patterns [94–97, 106, 107]. Positive feedback reflects the local enrichment of resources, where vegetation actively improves the sur-

rounding environment through physiological and ecological processes, thereby promoting its growth and that of nearby vegetation. For example, plant root systems can enrich soil moisture, reduce surface runoff, and enhance water retention capacity. This mechanism leads to the aggregation of water resources locally, creating a positive loop that facilitates the lush growth of vegetation. Additionally, vegetation can increase local soil nutrient content through the accumulation of litter, further driving the spatial clustering of vegetation. Vegetation can also reduce evaporation rates and modify the microclimate by shading the surface, thereby enhancing regional suitability and reinforcing the stability of vegetation patches. This positive feedback effects often exhibit high nonlinearity, where increases in vegetation density significantly enhance local resource availability. In mathematical models, this amplifying effect of positive feedback is often represented by nonlinear growth terms. For instance, in the Klausmeier model, the term wn^2 represents the positive feedback of vegetation on water resources, a similar formulation widely adopted in more complex models like the Rietkerk and Gilad models [36, 55, 84]. There, w and n are the water density and vegetation biomass, respectively. The essence of positive feedback lies in driving the local enrichment of resources, forming "hotspots" areas, and providing conditions for further vegetation expansion. However, relying solely on positive feedback can lead to excessive resource concentration and ecosystem instability. For example, systems that depend entirely on positive feedback may experience rapid vegetation degradation or collapse when resources are depleted.

To counterbalance the intensifying effects of positive feedback, negative feedback mechanisms regulate the expansion of vegetation through resource competition and diffusion processes. Negative feedback primarily limits vegetation expansion in high-density areas while redistributing resources to low-density regions, thereby maintaining the dynamic balance of system. For example, the Rietkerk model employs a nonlinear saturation function, such as $w/(w+k_1)$, to describe the limitation of water availability on vegetation growth [41, 84]. Namely, it grows approximately linearly when w is small but gradually saturates as w becomes large, approaching its maximum value asymptotically. The parameter k_1 determines the half-saturation threshold, i.e. the water level at which growth reaches half of its maximum rate. This resource competition becomes more pronounced with increasing vegetation density, ultimately suppressing disorderly expansion. In addition, diffusion processes redistribute resources across spatial gradients, further modulating the effects of local positive feedback. In mathematical models, the diffusion effects are commonly represented by terms such as $D_n\nabla^2 n$, where D_n is the diffusion coefficient and $\nabla^2 n$ describes the spatial redistribution of vegetation biomass, smoothing local density differences and preventing over-aggregation.

The synergistic interaction between positive and negative feedback mechanisms determines the formation conditions and stability of vegetation patterns. In reaction-diffusion models, positive feedback drives the emergence of patterns through local growth terms, while negative feedback maintains system stability through diffusion and resource competition terms. For instance, in the Rietkerk model, the interactions between vegetation, soil water and surface runoff are described by the following equations [41, 84]:

$$\begin{cases} \dfrac{\partial n}{\partial t} = cg_{\max}\dfrac{w}{w+k_1}n - mn + D_n\nabla^2 n, \\ \dfrac{\partial w}{\partial t} = \alpha\dfrac{n+k_2 f}{n+k_2}h - \nu w - \gamma\dfrac{w}{w+k_1}n + D_w\nabla^2 w, \\ \dfrac{\partial h}{\partial t} = p - \alpha\dfrac{n+k_2 f}{n+k_2}h + D_h\nabla^2 h, \end{cases} \tag{2.1}$$

where n, w and h are vegetation biomass, soil water, and surface water, respectively. The parameter $g_{\max}$ denotes the maximum specific growth rate, and k_1 is the half-saturation constant for water-limited growth. The growth term $cg_{\max}w/(w+k_1)n$ captures local positive feedback, as vegetation enhances its own growth under sufficient soil moisture. The mortality term $-mn$ reflects local negative feedback through natural death of vegetation, while the diffusion term $D_n\nabla^2 n$ introduces spatial negative feedback by smoothing biomass gradients. In the soil water equation, the term $\alpha(n+k_2 f)h/(n+k_2)$ represents infiltration of surface water, modulated by vegetation presence. Here, f quantifies the infiltration contrast between vegetated and bare-soil, k_2 determines the sharpness of this contrast, and α is the maximum infiltration rate. This infiltration term enhances positive feedback, as vegetation improves local infiltration, thereby increasing water availability. The terms $-\nu w$ and $-\gamma w/(w+k_1)n$ account for evaporation (with rate ν) and plant water uptake (with efficiency γ), respectively, both contributing to negative feedback by depleting soil water. The diffusion term $D_w\nabla^2 w$ redistributes soil moisture across space. In the surface water equation, rainfall enters at a constant rate p, and water is lost through infiltration $-\alpha(n+k_2 f)h/(n+k_2)$, coupled to the vegetation distribution. The diffusion term $D_h\nabla^2 h$ models overland water flow, which acts as a spatial stabilizing force. Together, the model captures a balance of positive feedbacks (e.g. vegetation-facilitated infiltration and growth) and negative feedbacks (e.g. mortality, evaporation, diffusion), which collectively drive the emergence and maintenance of spatial vegetation patterns in semi-arid ecosystems.

As research advances, models based on positive and negative feedback mechanisms have evolved to describe complex ecological processes and environmental impacts more precisely. Early models often assumed localized resource redistribution, while real-world ecological processes frequently exhibit significant nonlocality. Nonlocal processes include nonlocal diffusion and nonlocal competition [13, 27]. Nonlocal diffusion typically describes the lateral movement of water or resources, such as the long-distance movement of water along the surface or underground. Nonlocal competition reflects the profound effects of vegetation root systems, where plants in one area may extract water from another area via roots. These processes can be modeled using integral kernel functions. For example, the Gilad model introduces nonlocal effects of root systems through kernel functions $g(X,X',T)$, where the nonlocal terms can be expressed as [36]

$$G_n = \nu\int_\Omega g(X,X',T)w(X',T)\mathrm{d}X', \quad G_w = \gamma\int_\Omega g(X',X,T)n(X',T)\mathrm{d}X',$$

indicating that vegetation-water interactions are shaped not only by local conditions but also by the spatial reach of root systems. G_n aggregates the water that a plant at X can mobilize via its laterally spreading roots: moisture at surrounding locations X' contributes to growth at X in proportion to how easily the root system can reach X'. Hence, G_B is an effective supply term produced by root-mediated access to the neighborhood water field. G_W quantifies the cumulative water demand at location X imposed by vegetation located elsewhere. This is expressed via the kernel function $g(X',X,T)$, which measures how effectively roots from surrounding biomass at X' can access water at X. Thus, G_W serves as a nonlocal sink term, reflecting competitive water uptake driven by the spatial extent of root systems. A convenient and biologically interpretable choice for the kernel g is a Gaussian kernel whose width grows with local biomass (larger plants explore a wider soil domain) [36,74]

$$g(X,X',T)=\frac{1}{\pi S_0^2}\exp\left[-\frac{|X-X'|^2}{S[n(X,T)]^2}\right],$$

where $S(n)=S_0(1+En)$ is the lateral root-zone radius as a function of above-ground biomass (with $S_0=S(0)$ the seedling value). As $n(X,T)$ grows, $S(n)$ expands, so more distant soil contributes positively to G_n and, symmetrically, more neighbors can withdraw water at X via G_w. Positive feedback therefore extends the range of water capture through root proliferation, whereas nonlocal negative feedback limits excessive resource concentration through remote competition. The development and characteristics of classical feedback-based models are summarized in Table 1, which details their core equations, features, and applications.

The positive and negative feedback mechanisms not only influence resource distribution and system stability through spatial processes but also exhibit complexity through delayed effects in temporal dynamics (Fig. 1) [126]. Fig. 1 intuitively illustrates the differences in ecosystem responses to external disturbances under conditions with and without time delays. In the absence of delays, dynamic feedback allows the system to rapidly stabilize. However, when time delays are present, feedback lags can destabilize the system, leading to periodic oscillations or even collapse. This figure clearly demonstrates the profound impact of time delays on positive and negative feedback mechanisms.

In vegetation systems, dynamic behaviors are often influenced by time delays in resource utilization and environmental changes [122]. For instance, the processes of resource absorption, growth, and feedback in vegetation are not immediate but require a finite time. Such time delays can be expressed using delayed differential equations, becoming an important extension in describing the spatiotemporal dynamics of ecosystems under positive and negative feedback mechanisms. The general form of a delay model can be written as

$$\frac{\partial n}{\partial t}=f(n(t-\tau))+\nabla^2 n,$$

where τ represents the delay, reflecting the response lag of vegetation to environmental changes. This formulation enables more accurate simulations of the long-term impacts

Table 1: Classic vegetation-water models based on positive and negative feedback mechanisms.

Name	Equations	Key features and innovations	Refs.
Lefever-Lejeune model (1997)	$\frac{\partial n}{\partial t}=(1-\mu)n+(\Lambda-1)n^2-n^3 +\frac{1}{2}(L^2-n)\nabla^2 n-\frac{1}{8}n\nabla^4 n.$	Single-variable model, describing local positive feedback and remote negative feedback, used for capturing regular vegetation patterns.	[58]
Klausmeier model (1999)	$\frac{\partial n}{\partial t}=wn^2-mn+\Delta n,$ $\frac{\partial w}{\partial t}=p-w-wn^2+v\nabla w.$	Introduces water as a dynamic variable, emphasizing the role of water-vegetation positive feedback, revealing the conditions for vegetation pattern formation.	[55]
von Hardenberg model (2001)	$\frac{\partial n}{\partial t}=\frac{\gamma w}{1+\sigma w}n-n^2-mn+\Delta n\frac{\partial w}{\partial t}$ $=p-(1-\rho n)w-w^2n +\delta\Delta(w-\beta n)-v\nabla(w-\alpha n).$	First to introduce cross-diffusion terms, revealing vegetation's competition for water resources and predicting transitions from bare soil at low precipitation to homogeneous vegetation at high precipitation.	[118]
Rietkerk model (2002)	$\frac{\partial n}{\partial t}=cg_{max}\frac{w}{w+k_1}n-mn+D_n\nabla^2 n,$ $\frac{\partial w}{\partial t}=\alpha\frac{n+k_2 f}{n+k_2}h-vw-\gamma\frac{w}{w+k_1}n +D_w\nabla^2 w,$ $\frac{\partial h}{\partial t}=p-\alpha\frac{n+k_2 f}{n+k_2}h+D_h\nabla^2 h.$	Expands water dynamics by introducing layers of surface and soil water, emphasizing the balance between positive and negative feedback.	[41], [84]
Gilad model (2004)	$\frac{\partial n}{\partial t}=G_n n(1-n)-n+D_n\Delta n,$ $\frac{\partial w}{\partial t}=Ih-v(1-\rho n)w-G_w w +D_w\Delta w,$ $\frac{\partial h}{\partial t}=p-Ih+D_h\Delta h.$	Incorporates nonlocal feedback mechanisms, combining root-level competition and lateral water flow, significantly increasing model complexity.	[35], [36]
Simplified Gilad model (2015)	$\frac{\partial n}{\partial t}=vwn(1-n)(1+\eta n)^2 -n+D_n\Delta n,$ $\frac{\partial w}{\partial t}=Ih-v(1-\rho n)w -\gamma(1+\eta n)^2 wn+D_w\Delta w,$ $\frac{\partial h}{\partial t}=p-Ih+D_h\Delta h.$	Reveals the mechanism of spatial self-organization in the formation of Australian fairy circles.	[130], [34]

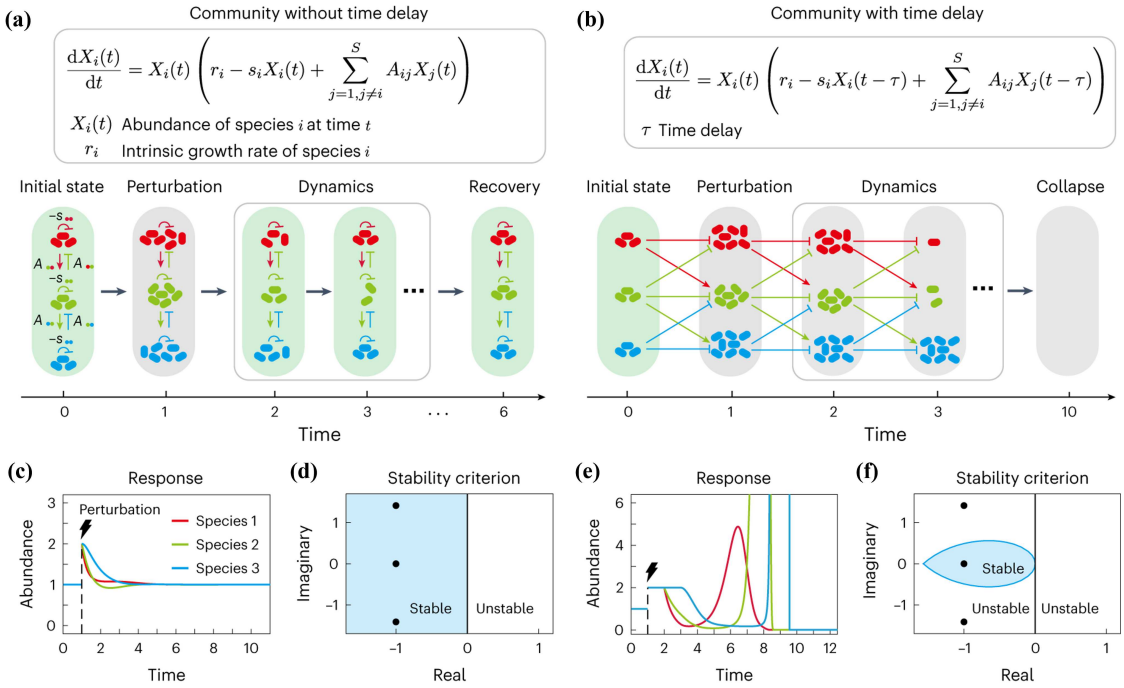

Figure 1: Illustration of ecosystem dynamics with and without time delays. (a) In the absence of time delays, species interactions occur instantaneously, allowing for rapid stabilization following perturbations, as seen in the progression from the initial state through recovery. (b) When time delays are introduced, interactions are temporally lagged, leading to prolonged dynamic responses and potential destabilization, culminating in ecosystem collapse. (c), (e) Abundance trajectories of three interacting species demonstrate smooth recovery in the delay-free system versus oscillatory behavior and instability in the delayed system. (d), (f) Stability regions in the complex plane reveal that time delays can shift system eigenvalues from a stable regime to an unstable regime, emphasizing the critical role of delays in determining ecological stability. Source: Adapted from [126].

of climatic events on ecosystems, such as droughts and rainfall, and reveals the temporal dynamics of vegetation during catastrophic shifts and recovery processes.

The delay effects not only alter the temporal responses of vegetation systems but also influence the dynamic behavior of patterns through coupling with diffusion processes. When there is a delay in the response of vegetation to changes in water or nutrient availability, studies have shown that this time delay can disrupt the equilibrium state of the system, leading to periodic oscillations in patterns. Li *et al.* [59] applied delay effects to describe the time difference in vegetation growth following water absorption, coupling this delay effect into an extended Klausmeier model, and obtained

$$\begin{cases} \dfrac{\partial N}{\partial t} = RJW(x,t-\tau)N^2(x,t-\tau) - MN(x,t) + D_1\nabla^2 N(x,t), \\ \dfrac{\partial W}{\partial t} = P - LW(x,t) - RW(x,t)N^2(x,t) + D_2\nabla^2\big(W - \beta_1 N(x,t)\big). \end{cases} \tag{2.2}$$

Li *et al.* [59] analysis shows that when the contribution of water to vegetation growth involves a time delay, the system may no longer maintain a stationary equilibrium but

instead enter a state of periodic oscillation . This dynamic feature not only alters the temporal behavior of vegetation but may also affect pattern formation by disrupting spatial uniformity, causing the vegetation system to exhibit more complex dynamic behavior. Furthermore, the effects of time delays in ecosystems also play a role in a large spatial range. The response of vegetation to long-distance resource changes is often subject to longer delays, such as the transmission time of groundwater resources in different regions or the competitive processes of plant root over large areas. This long-range delay can be described mathematically using nonlocal integral terms, such as [46]

$$\begin{cases} \dfrac{\partial N}{\partial t} = RJN^2 \displaystyle\int_\Omega \int_{-\infty}^{t} I(x,y,t-\tau)B(t-\tau)W(y,\tau)\mathrm{d}\tau\mathrm{d}y - MN + D_1\nabla^2 N(x,t), \\ \dfrac{\partial W}{\partial t} = P - LW - RN^2 \displaystyle\int_\Omega \int_{-\infty}^{t} I(x,y,t-\tau)B(t-\tau)W(y,\tau)\mathrm{d}\tau\mathrm{d}y + D_2\nabla^2(W-\beta_1 N), \end{cases} \tag{2.3}$$

where $I(x,y,t-\tau)$ is a spatial kernel function that describes how vegetation at location x is influenced by water availability at location y with a delay $t-\tau$, and $B(t-\tau)$ is a memory kernel that represents the temporal influence or efficiency of delayed water uptake. The study by Hou *et al.* [46] reveals that the combination of time delays and long-range effects can increase the complexity of vegetation patterns, potentially transforming regular patterns into more heterogeneous structures, such as quasiperiodic or fractal patterns. This complexity manifests not only in the spatial distribution of vegetation but also in nonlinear transitions of vegetation from one stable state to another.

Moreover, the intensification of global climate change has brought new challenges and directions to the study of vegetation patterns. Climate factors, such as precipitation intensity, evaporation rates, and temperature fluctuations, not only alter the temporal dynamics of ecosystems but also influence the formation and evolution of patterns through their complex interactions with positive and negative feedback mechanisms [20, 54, 103]. Long-term trends and short-term fluctuations driven by climate change often regulate the core dynamical processes of vegetation growth through various pathways. For example, reduced precipitation or increased evaporation may directly weaken positive feedback mechanisms, preventing vegetation from effectively concentrating water resources. Simultaneously, temperature fluctuations may indirectly alter the physiological and metabolic processes of plants, thereby affecting their competitive ability and resource utilization efficiency. The work by Kefi *et al.* [54] incorporated climate factors (particularly atmospheric CO_2 concentrations) into vegetation models, significantly advancing the understanding of the complexity of arid ecosystems. By integrating key climatic drivers CO_2 concentrations, temperature, and precipitation into the framework of positive and negative feedback mechanisms, the study elucidates how these factors regulate vegetation growth, transpiration efficiency, and resource cycling. The core equations of their model are expressed as follows:

$$\frac{\partial P}{\partial t} = c\alpha_2 g_{CO_2} \frac{W}{W+k_1} P - R_{esp}P + D_p\Delta P, \tag{2.4a}$$

$$\frac{\partial W}{\partial t}=\alpha O\frac{P+k_2W_0}{P+k_2}-\alpha_2\gamma g_{CO_2}\frac{W}{W+k_1}qP-r_wW+D_w\Delta W, \tag{2.4b}$$

$$\frac{\partial O}{\partial t}=R-\alpha O\frac{P+k_2W_0}{P+k_2}+D_o\Delta O \tag{2.4c}$$

with

$$c=C_a\left(1-\frac{C_i}{C_a}\right)C_1,\quad R_{esp}=R_bQ_{10}^{\frac{T-10}{10}},\quad q=q^*-q_a=\frac{0.622}{p}e^*(1-Rh).$$

Simulation results show that increased CO_2 concentrations can enhance vegetation survival by improving water use efficiency (g_{CO_2}) and reducing transpiration rates, thereby improving overall ecosystem stability. Under high CO_2 conditions, the system tends to form more stable and denser vegetation patterns. However, in scenarios with low precipitation, the scarcity of water resources may outweigh the benefits of increased CO_2, potentially leading to vegetation degradation or transitions from regular patterns to sparse distributions or even desertification. Furthermore, the study by Kefi *et al.* [54] reveals the complex coupling between climatic factors and internal ecosystem feedback mechanisms, which significantly influence the dynamics and stability of vegetation patterns. With intensified climate change, vegetation patterns may evolve from regular distributions to more heterogeneous or sparse configurations, while driving ecosystems toward nonlinear transitions between different stable states. By integrating climatic factors with the framework of positive and negative feedback mechanisms, the model (2.4) deepens our understanding of the formation and evolution of vegetation patterns under climate change. It also provides a crucial theoretical framework for predicting the impacts of global climate change on arid ecosystems and emphasizes the importance of monitoring climate drivers (such as CO_2, precipitation, and temperature changes) to assess ecosystem stability.

2.2 Multistable phenomena and stability

Multistability is a critical characteristic of ecosystem dynamics, referring to the ability of a system to maintain multiple stable states under identical external conditions, such as states with high vegetation density, low vegetation density, or bare soil. This phenomenon is particularly significant in the formation and maintenance of vegetation patterns, reflecting the inherent complexity of ecosystems and their resilience under environmental changes. The formation and dynamic characteristics of multiple stable states, as well as their impact on ecosystem stability, constitute the key content for understanding the relationship between vegetation patterns and ecosystem stability. Multistability arises from the interplay of positive and negative feedback mechanisms within ecosystems, driven by nonlinear ecological processes such as localized resource enrichment, diffusion constraints, and competitive interactions. These processes enhance the nonlinear properties of the system, allowing ecosystems to exhibit varying stability and resilience under changing environmental conditions. To gain deeper insights into multi-

stability and its impact on ecosystem stability, researchers have extensively explored its mechanisms, dynamics, and behavior under various environmental conditions through theoretical models and field observations [90, 105, 127].

Theoretical models and field studies have consistently confirmed the prevalence of multistability and provided mathematical and visual tools to explain catastrophic shifts in ecosystems. For example, the research by Scheffer *et al.* [90] demonstrates that multistable behavior in ecosystems is often accompanied by the presence of tipping points. They proposed the concepts of the folded equilibrium curve and hysteresis loop, which offer a theoretical foundation for predicting regime shifts (Fig. 2). Fig. 2(a) illustrates a classic fold bifurcation structure, in which an ecosystem exhibits multiple stable states under gradually changing environmental conditions. The curve shows how the system state responds nonlinearly to variations in an external driver. Stable branches are shown as solid lines, while unstable branches are indicated by dashed lines.

As conditions deteriorate, the system gradually moves along the upper stable branch until it reaches a critical tipping point (F_2), where a small change leads to a abrupt transition to a lower stable state, known as a forward shift. When conditions are reversed,

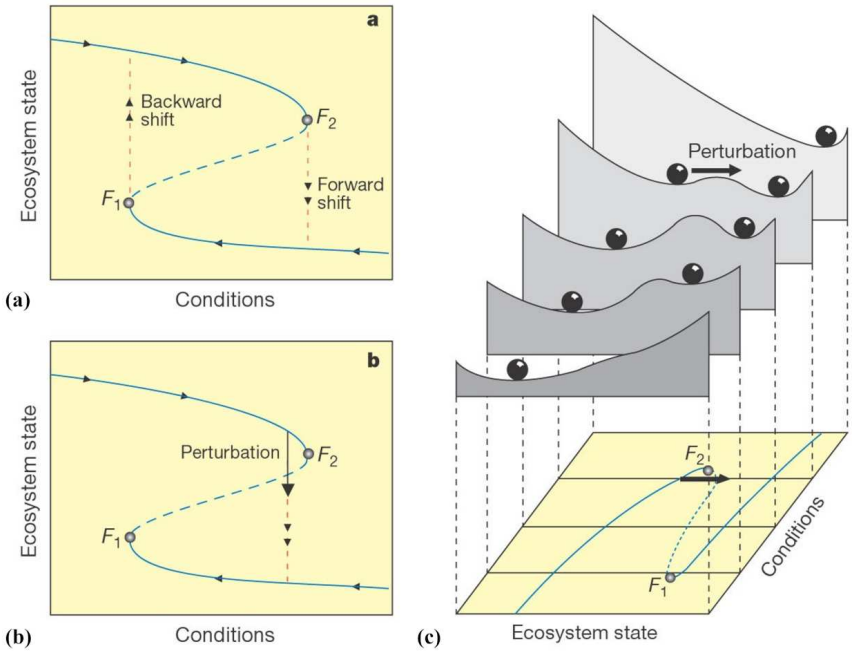

Figure 2: Illustrations of ecosystem state shifts and stability landscapes under varying conditions. (a) The folded equilibrium curve highlights forward (F2) and backward (F1) shifts between ecosystem states as external conditions (e.g. resource availability) change. Solid lines represent stable states, while dashed lines indicate unstable states. (b) External perturbations near the folded equilibrium curve can drive abrupt state transitions, emphasizing the sensitivity of ecosystems close to tipping points. (c) Stability landscapes represent ecosystem states as valleys (stable equilibria) and hills (unstable equilibria), with changes in external conditions affecting the basin of attraction. Perturbations can push the system between stable states, illustrating the interplay between stability and resilience in multi-stable ecosystems. Source: Adapted from [90].

the system does not return to its original state immediately. Instead, it remains in the altered state until it reaches a second threshold (F_1), where a backward shift occurs. This hysteresis behavior reflects the influence of positive feedback mechanisms that maintain the system within a given regime and resist change until critical points are crossed. Fig. 2(b) depicts how external disturbances directly affect system states. When the system approaches the folded curve, even small perturbations can push it into another stable state, highlighting its high sensitivity near critical conditions. Additionally, Fig. 2(c) uses a landscape representation to illustrate stability: valleys represent stable states, while ridges indicate unstable states. As external conditions change or perturbations increase, the system may transition from one stable state to another. This landscape model reflects the size of attractor basins and their resilience to disturbances. For instance, smaller attractor basins imply that even moderate disturbances can push the system into other stable states. This increasing vulnerability to perturbations, especially as the system approaches a bifurcation point, emphasizes the importance of identifying early warning signals for regime shifts in multistable systems.

Building on this theoretical foundation, von Hardenberg *et al.* [118] predicted the multistable characteristics of vegetation systems under varying precipitation conditions using constructed models. When precipitation approaches a critical threshold, the system may abruptly shift from a high vegetation cover state to a low vegetation cover or bare soil state [85]. Such catastrophic shifts are driven by positive feedback mechanisms: under resource-limited conditions, the ability of vegetation to enrich water diminishes, further reducing resource availability, ultimately degrading the system into a bare soil state. These shifts are described as catastrophic bifurcations, mathematically characterized by abrupt changes in solutions when system parameters reach a critical threshold. Fig. 3 provides a detailed illustration of this catastrophic bifurcation and the specific manifestations of multistability. There, the horizontal axis represents resource input (e.g. precipitation), and the vertical axis represents ecosystem states (e.g. vegetation biomass). Solid parts of the curve indicate stable states, while dashed parts represent unstable states. Changes in resource input, from high to low, reflect the potential state transitions of the system: from uniform vegetation to patterned vegetation and eventually to bare soil. Notably, in the range $[p_0, p_1]$, the system exhibits significant multistability, where it can maintain a uniform vegetation, patterned vegetation, or bare soil state, depending on initial conditions or external disturbances.

To further explore the complexity of multistability, Zelnik *et al.* [127] focused on tristability, which includes uniform vegetation (UV), periodic patterns (PP), and bare soil (BS) states. Their research demonstrates that these states not only exist independently under specific conditions but can also exhibit dynamic transitions influenced by complex interactions between feedback mechanisms and disturbances (Fig. 4). For example, under low-intensity disturbances, the system may oscillate between two adjacent stable states. However, with increased disturbance intensity, the system may transition to a completely different stable state. These phenomena are jointly driven by feedback mechanisms and environmental parameters. Fig. 4 provides a clear visualization of the transitions among

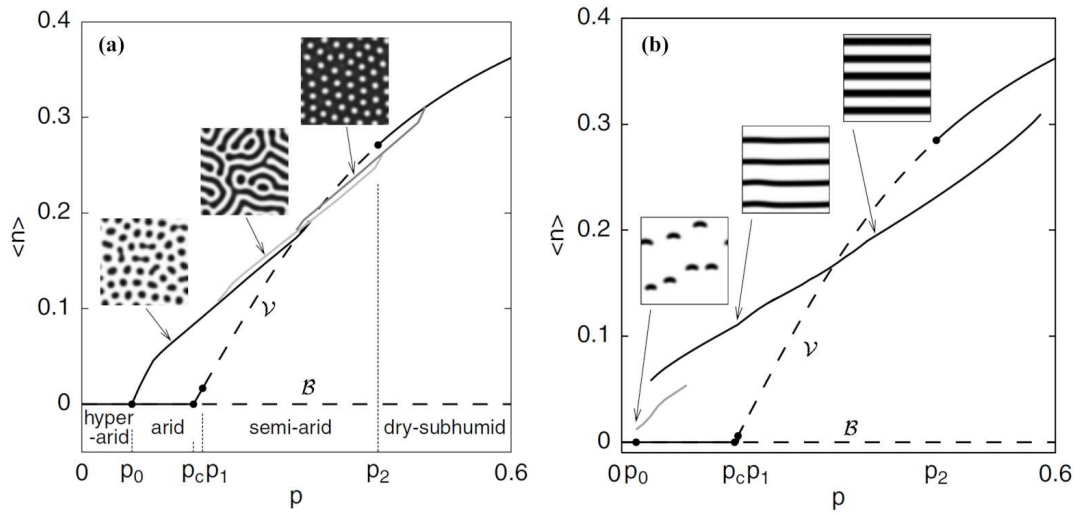

Figure 3: (a) and (b) show the averaged density of vegetation biomass (n) versus rainfall (p) under different slope conditions. (a) represents flat terrain, while (b) incorporates finite slope. Solid lines indicate stable equilibria, and dashed lines represent unstable states. Insets illustrate vegetation patterns, highlighting transitions such as spotted, labyrinthine, and homogeneous states as resource input changes. The influence of slope shifts stability boundaries and modifies vegetation patterns. Source: Adapted from [118].

these states and their distribution within the parameter space. The bifurcation diagrams in the upper row of Fig. 4(a) reveal the stability regions and boundaries of UV, PP, and BS states. Black curves represent the stable regions of UV and BS states, blue curves indicate PP states, and red curves highlight localized hybrid states such as BS & UV, UV & PP, and PP & BS. The spatial distribution diagrams in the lower row of Fig. 4(a) further illustrate vegetation (green) and water (blue) spatial patterns under specific parameters. For example, direct transitions between UV and BS indicate desertification processes, while localized hybrid states between UV and PP suggest that patterned vegetation can act as a transitional state. Within the serpentine region, hybrid states between UV and PP are stable, allowing the system to maintain complex front or patch structures. Fig. 4(b) presents a stability parameter diagram that further characterizes the stable regions and boundary features of different states within the parameter space defined by precipitation (a) and diffusion coefficient (d). These boundaries delineate the critical conditions under which the system transitions from one stable state to another. Fig. 4(c) illustrates the spatiotemporal dynamics of the system under various parameter conditions. For example, under low diffusion conditions (e.g. point A in the right figure of Fig. 4(b)), the bare soil state can invade the uniform vegetation state, leading to desertification. Conversely, under high diffusion conditions (e.g. point F in the right figure of Fig. 4(b)), the system is more likely to transition from UV to PP, where diffusion facilitating the formation of periodic patterns. Under intermediate conditions (e.g. point C in the right figure of Fig. 4(b)), the system may maintain a mixed state where UV, PP, and BS alternate, resulting in complex dynamic behaviors.

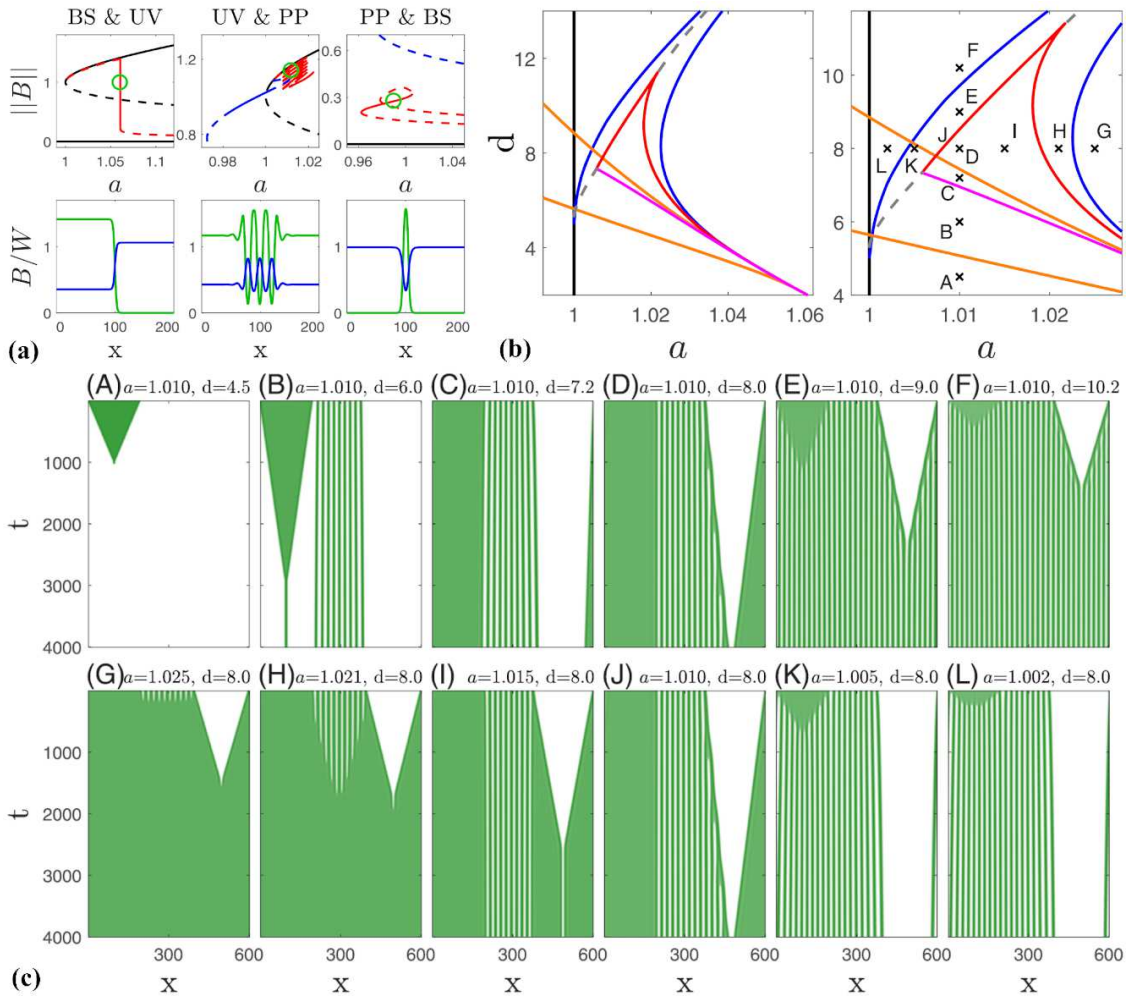

Figure 4: Dynamics of tristability in vegetation patterns. (a) Stability diagrams showing the coexistence of bare soil, uniform vegetation, and periodic patterns under varying control parameters (e.g. rainfall a). The bottom row illustrates spatial distributions of biomass (B) and water (W) corresponding to different stable states. (b) Parameter space highlighting stability regions for different states and their bifurcations. The left plot shows regions of stability for UV, PP, and BS states under varying rainfall (a) and diffusion (d), while the right plot identifies specific parameter points (A-L) corresponding to multistable states. Snake-like structures indicate regions of multistability, where combinations of BS & UV, UV & PP, or PP & BS coexist under certain conditions. (c) Spatiotemporal dynamics corresponding to the parameter points (A-L) in (b, right). Each subpanel (A-L) illustrates how vegetation patterns evolve over time and space under specific parameter settings, demonstrating transitions, oscillations, or coexistence between different stable states. Source: Adapted from [127].

Building on this, Xue *et al.* [124] developed a vegetation-water model with nonlocal water uptake to investigate how root-mediated competition influences multistability transitions. Their weakly nonlinear analysis revealed that the strength of nonlocal uptake can alter the nature of Turing bifurcations: under low water diffusivity, stronger nonlocal

effects shift the system from supercritical to subcritical bifurcations, thereby inducing homoclinic snaking structures and localized states. Numerical simulations further showed that as precipitation varies, the system undergoes a sequence of stability transitions: from monostability (bare soil), to bistability, to tristability (coexistence of BS-UV-PP), and back to bistability (Fig. 5). Under subcritical conditions, a rich set of localized hybrid states, such as single-peak (Fig. 5(i)) and multi-peak (Fig. 5(h)) structures. Moreover, by comparing vegetation patterns in Senegal and Australia, the study demonstrated that differences in nonlocal uptake intensity – linked to soil texture and root system architecture – can explain regional contrasts: strong nonlocal uptake in sandy soils favors the formation of regular fairy circles, while weaker uptake in clay soils promotes irregular or mixed patterns. These findings highlight the critical role of nonlocal interactions in driving multistability and provide a theoretical framework to interpret observed spatial heterogeneity across dryland ecosystems.

Recent work has further extended the understanding of multistability by revealing that reaction-diffusion systems can even support the coexistence of three fundamentally

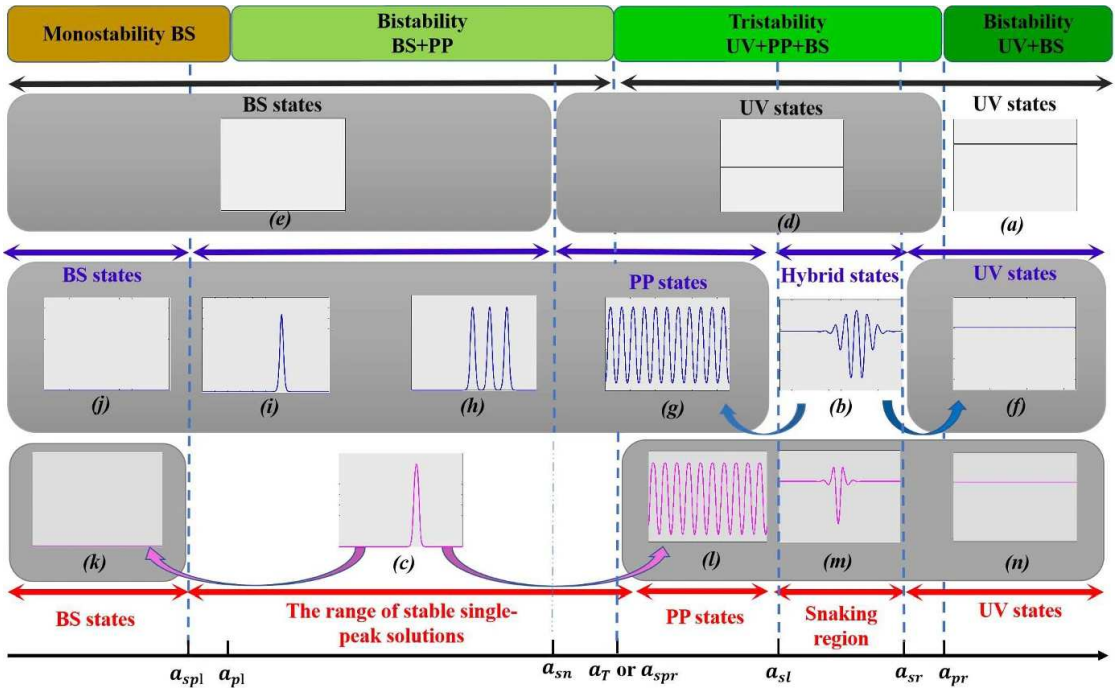

Figure 5: Shifts of multiple vegetation states in the vegetation-water model with nonlocal uptake. The precipitation axis is divided into four intervals by critical thresholds (a_{pl},a_T,a_{pr}), corresponding to monostability of bare soil, bistability of BS+PP, tristability of UV+PP+BS, and bistability of UV+BS. Row (a,d,e): Starting from UV (a), vegetation density decreases with precipitation until it collapses irreversibly to BS when $a < a_{sn}$. Row (f,b,g,h,i,j): Starting from a hybrid UV-PP state (b), increasing precipitation drives the system to UV, while decreasing precipitation induces PP, multi-peak and single-peak states, eventually collapsing to BS. Row (c,k,l,m,n): Starting from a single-peak state (c), the system shifts to BS under drought and recovers back to UV under rainfall increase, passing through PP and hybrid states. Source: Adapted from [124].

distinct states, a phenomenon described as three-domain chimera states [105]. Specifically, this study demonstrated that when zero-uniform (ZU), non-zero-uniform (NZU), and periodic patterned states simultaneously coexist, the system exhibits a novel form of tristability beyond classical ecological cases. The emergence of such states requires three mathematical conditions: (i) bistability between ZU and NZU accompanied by the presence of a Maxwell point, (ii) a subcritical Turing bifurcation of one of the uniform states leading to coexistence with PP, and (iii) the occurrence of a homoclinic snaking structure at the Maxwell point. Under these conditions, the ZU, NZU, and PP states can stably coexist, giving rise to a stationary three-domain chimera; deviations from the Maxwell point, however, cause the structure to collapse into classical two-domain chimeras. Importantly, this mechanism has been validated across several canonical models, including the generalized Swift-Hohenberg, extended Klausmeier, and Guttal-Jayaprakash models, underscoring the universality of tristability phenomena in spatially extended systems. These findings provide a strong theoretical complement to ecological studies, highlighting the deep connection between mathematical multistability and the resilience or vulnerability of ecosystems under environmental stress.

These findings significantly expand the understanding of ecosystem responses to environmental changes, providing more complex transition pathways compared to traditional bistability. For instance, in the face of drought or grazing disturbances, the system may delay complete degradation to bare soil by maintaining localized hybrid states. The patch structures within the serpentine region provide resilience, allowing the system to adapt better to environmental disturbances. Furthermore, this phenomenon enriches the dynamics of vegetation patterns and offers new perspectives for ecosystem management. In tristable systems, human interventions that limit bare soil expansion while maintaining patterned vegetation can significantly enhance ecosystem stability. This approach is particularly crucial for semi-arid ecosystems, which often operate near critical thresholds under climate change and human disturbances.

Additionally, Bastiaansen *et al.* [4] validated the multistable characteristics of ecosystems by extending the Klausmeier model and proposed the concept of the "Busse Balloon" to describe the distribution of multiple stable states under different combinations of environmental parameters. In particular, within the Turing instability region, periodic patterned states with different wavelengths can emerge from distinct bifurcation points, resulting in multistability among modes of varying spatial scales [105]. As shown in Fig. 6, the bifurcation diagram and spatial distributions illustrate how decreasing values of the control parameter λ generate PP states with increasing wavelengths, while the amplitude of the steady-state solution oscillates before converging to a finite value. This indicates that ecosystems can sustain multiple patterned states simultaneously, depending on environmental conditions, and even supports chimera-like states characterized by the coexistence of patterns with different wavelengths (Fig. 6(a5)). Such findings emphasize that multistability not only occurs between homogeneous and patterned vegetation but also within patterned states themselves, enriching the spectrum of possible vegetation dynamics.

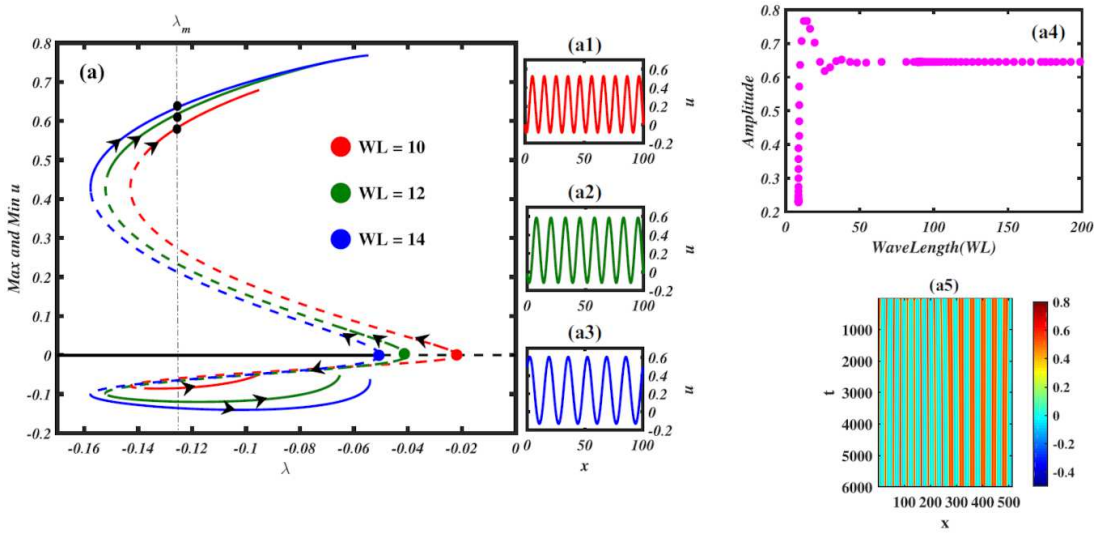

Figure 6: Periodic patterned states with different wavelengths at the Maxwell point within the Turing instability region. Bifurcation diagram showing the coexistence of multiple PP states originating at different bifurcation points. Panels (a1)-(a3) depict spatial patterns of PP states with increasing wavelength as the bifurcation parameter λ decreases. Panel (a4) shows how the amplitude of the solution oscillates before converging to a finite value with wavelength. Panel (a5) illustrates a chimera-like state characterized by the coexistence of two PP states with distinct wavelengths. Source: Adapted from [105].

Rietkerk *et al.* [83] identified the diversity of stable patterns within parameter spaces such as the Busse Balloon region, highlighting the adaptive capacity of ecosystems under stress. This diversity enables ecosystems to maintain their overall functionality and productivity by adjusting local or global patterns. The study further demonstrated that during disturbances, the formation of coexisting states allows ecosystems to sustain multiple stable states spatially rather than collapsing into a single state. This phenomenon is particularly evident in transitional zones between wet and arid environments. For example, in savanna ecosystems, multiple stable spatial patterns have been observed, including forest-grassland boundaries in wet areas, Turing patterns of sparse savanna and dry grassland in moderately wet areas, and grassland-desert patches in arid regions (Fig. 7). The coexistence of these patterns reflects the adaptive capacity and diversity of ecosystems. Particularly during rapid environmental changes, these diverse patterns provide buffer and recovery capacity for the ecosystem. Fig. 7 illustrates the typical distribution of these spatial patterns, revealing that their stability depends on environmental parameters (e.g. precipitation and diffusion coefficients) and the dynamic balance between local and global feedback mechanisms. For ecosystem management, this multistability offers significant insights: through interventions such as regulating resource allocation or vegetation types, the stability of ecosystems under varying environmental conditions can be enhanced, thereby reducing the risk of transitions to bare soil or low biomass states.

Multistability not only determines ecosystem stability but also characterizes resilience and vulnerability. On the one hand, systems with multistability can recover to original

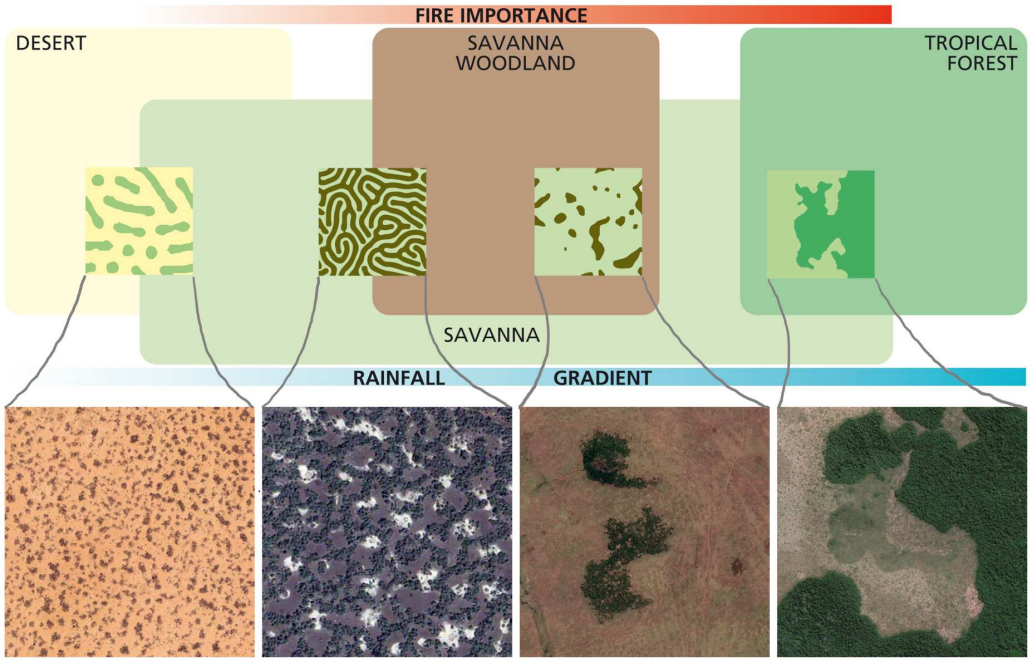

Figure 7: Representation of vegetation spatial patterns across varying environmental gradients. The top panel illustrates transitions between desert, savanna, and tropical forest ecosystems, influenced by factors such as fire intensity and rainfall. Insets depict characteristic vegetation structures: spots and stripes in arid regions, labyrinth-like patterns in savannas, and denser formations in humid zones. The bottom panel displays satellite images corresponding to these patterns, highlighting the ecological processes driving transitions and the role of spatial self-organization in ecosystem resilience. Source: Adapted from [83].

stable states under minor disturbances, providing resilience against short-term environmental changes. On the other hand, exceeding critical thresholds may lead to transitions to alternate stable states, with potential irreversibility. For instance, overgrazing or prolonged droughts may degrade vegetation into bare soil, worsening conditions and reducing recovery capacity. Overall, multistability plays a key role in the formation of vegetation patterns and ecosystem stability. Studying its mechanisms, thresholds, and transitions provides crucial insights into ecosystem dynamics under changing environments, supporting vegetation restoration and ecological conservation efforts.

3 Vegetation pattern and ecosystem resilience

Vegetation patterns not only serve as key indicators of ecosystem health but also play a critical role in system resilience and adaptive capacity. The formation and variation of these patterns reflect the stability and dynamic responsiveness of ecosystems to environmental disturbances. In semi-arid or degraded ecosystems, structural characteristics of vegetation patterns such as spacing, morphology, and spatial distribution not only act as diagnostic tools for assessing system states but also provide scientific insights into pre-

dicting ecosystem recovery potential and designing management strategies. This section will delve into the pivotal roles of vegetation patterns in the early warning of degradation, recovery processes, and ecosystem management.

3.1 Early warning signals

Vegetation patterns, as spatial representations of ecosystem states, reflect signals of systems approaching critical points, thus serving as important early warning signs for ecosystem degradation. In the context of intensified global climate change and human activities, ecosystems often exhibit localized nonlinear responses rather than uniform adjustments. Research has shown that such localized responses manifest as self-organized vegetation patterns, demonstrating evolution processes with complex dynamics. Traditional elasticity metrics often fail to capture these processes as they generally assume uniform ecosystem responses to changing environmental conditions until the system crosses a critical threshold and undergoes catastrophic transitions, neglecting spatial effects and pattern transitions. However, real-world ecosystems exhibit more complex self-organizing behaviors due to spatial heterogeneity, forming localized patch patterns that not only represent ecosystem steady states but also carries the rich dynamic information about the system. As a result, changes in vegetation patterns have become central to studying ecosystem degradation. By analyzing the shape, distribution, and dynamics of patterns, signals of critical thresholds can be identified, providing early guidance for management interventions. These early warning signals mainly manifest in the following aspects:

- **Increase in patch spacing**: As ecosystems approach critical thresholds, the spacing between vegetation patches often increases significantly. This is due to the increased heterogeneity in resource distribution within the system, leading to sparser vegetation distribution. Changes, especially the increase in patch spacing, are widely regarded as key indicators of declining system stability [3].
- **Irregularity in shape**: Under unfavorable environmental conditions, vegetation patterns gradually shift from regular to irregular distributions, characterized by blurred boundaries and fragmented patches [51–53]. This irregularity reflects the weakening of positive feedback mechanisms and the strengthening of negative feedback mechanisms, marking significant ecosystem degradation.
- **Critical slowing down**: As ecosystems approach critical thresholds, their response speed to external disturbances decreases significantly, and recovery time increases dramatically [88]. This dynamic behavior indicates a gradual loss of self-regulating capacity within the system.

These features collectively demonstrate the characteristics of vegetation patterns as systems near critical points. Both theoretical models and field observations have validated the effectiveness of vegetation patterns as early warning signals of ecosystem degrada-

tion, revealing the mechanisms and applicability of these signals. Below, we delve into the details using theoretical models and field observations.

3.1.1 Patch spacing as a key early warning signal

The increase in patch spacing, a significant early warning signal, is often explained by reaction-diffusion models. In such models, the interplay between localized resource accumulation and diffusion constraints leads to spatial patterns with specific wavelengths. As systems approach critical points, decreased resource weakens positive feedback mechanisms, extending the wavelength of patterns. For instance, the Klausmeier and Gilad models indicate that when precipitation falls below a certain threshold, vegetation patch spacing increases rapidly [77, 106]. This phenomenon has been empirically validated in dryland vegetation systems, particularly in semi-arid savannas, where significant increases in patch spacing align closely with trends of ecosystem degradation [6,70,83].

From a dynamic perspective, as precipitation decreases, the feasible region – defined as the subset of system configurations that can maintain stable vegetation patterns under given environmental conditions – progressively shrinks, resulting in larger vegetation patch spacing and eventual unsustainability (Fig. 8). Specifically, under high precipitation conditions, resource allocation within patch systems supports regular patch arrangements (Fig. 8(d)). However, as precipitation decreases, the feasible region of system gradually contracts, rendering some vegetation patches unsustainable and causing their disappearance (Figs. 8(e), 8(f)). This dynamic change manifests as an increase in patch spacing, with newly formed patch configurations becoming increasingly irregular. This process illustrates the direct impact of declining precipitation on patch spacing and further corroborates the significance of increasing patch spacing as an early warning signal of system degradation. From this perspective, the increase in patch spacing is a passive phenomenon, reflecting a reorganization of vegetation patches under environmental pressure. This reorganization is not only governed by resource distribution constraints but also influenced by the rate of environmental change. In scenarios of slow environmental change (blue lines in Figs. 8(b), 8(c)), vegetation patches have sufficient time to reorganize, redistributing resources among existing patches to form more regular structures. These regular configurations exhibit higher resilience, enabling stability under lower precipitation levels. However, with continued precipitation decline, the system eventually undergoes a "period-doubling" transition, where half of the patches disappear, signaling a shift to a more degraded state. In contrast, under rapid environmental change (red lines in Figs. 8(b), 8(c)), patches lack the time needed for self-reorganization. As the feasible configuration region contracts rapidly, patches disappear one by one, eventually leading to desertification. This degradation pathway highlights the critical role of the rate of change in ecosystem stability and underscores how rapid changes typically result in more severe degradation patterns [3]. These observations further emphasize the value of patch spacing dynamics as a warning signal of ecosystem degradation while providing theoretical support for assessing whether the system is approaching a tipping point.

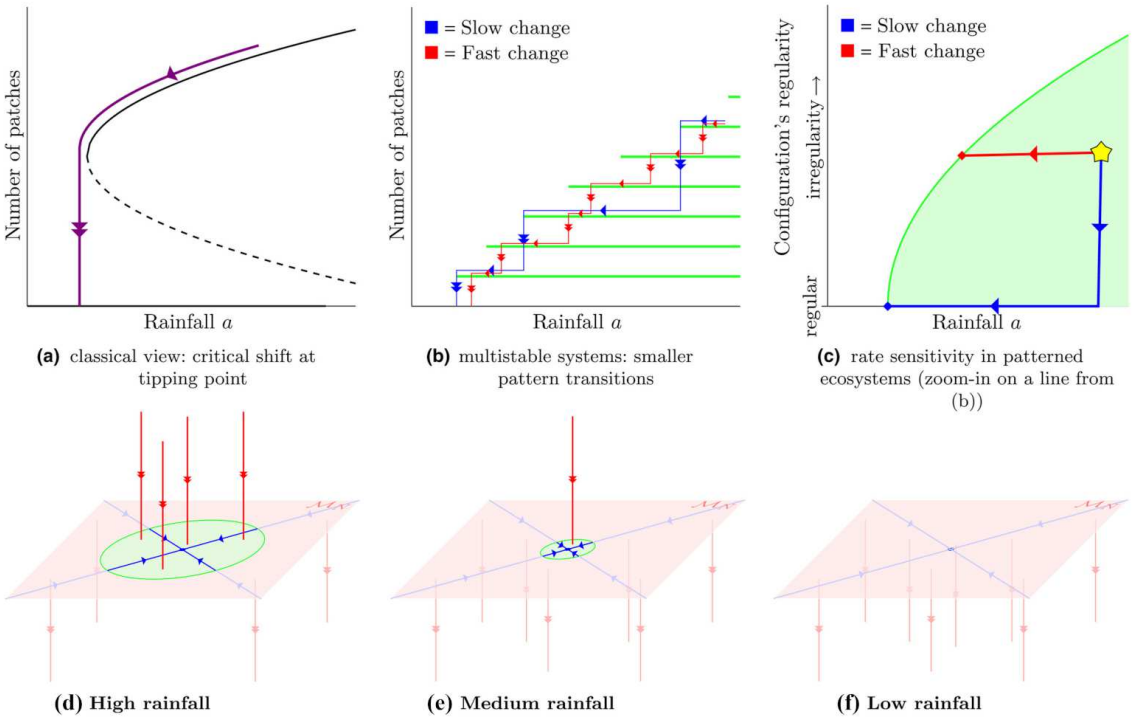

Figure 8: Illustration of ecosystem dynamics and sensitivity to rainfall changes in patterned ecosystems. (a) Classical perspective of critical transitions: Ecosystems exhibit abrupt shifts at tipping points as rainfall a decreases, characterized by a sudden drop in the number of patches (solid and dashed lines indicate stable and unstable states, respectively). (b) Multistable systems: Smaller pattern transitions occur as rainfall decreases. Slow environmental changes (blue lines) allow for smoother, stepwise reorganization of patches, while fast changes (red lines) lead to abrupt collapses with limited reconfiguration. (c) Sensitivity to rate of change: Regular configurations are more resilient under slow rainfall decreases (blue lines) but exhibit irregular transitions under rapid changes (red lines), highlighting the rate-dependence of ecosystem responses. (d)-(f) Conceptual phase portraits of patterned ecosystems under varying rainfall conditions. (d) High rainfall: Feasible configurations (green ellipse) support numerous patches. (e) Medium rainfall: Shrinking feasible region with fewer stable configurations; patches become more vulnerable and tend to collapse. (f) Low rainfall: Feasible configurations disappear; ecosystem dynamics favor widespread patch loss and transition to desertified states. Source: Adapted from [3].

3.1.2 Irregularity in shape and fragmentation

The irregularity in vegetation patterns reflects changes in the internal dynamics of the system. As external pressures such as overgrazing or climate change increase, the structure of vegetation patches gradually shifts from regular arrangements to irregular distributions. This transformation is often characterized by blurred patch boundaries, fragmentation, and disruptions in internal homogeneity. Research by Kéfi *et al.* [51–53] highlights that these morphological changes in patterns are closely tied to the scaling properties of ecosystems. In healthy ecosystems, vegetation patterns typically follow a power-law distribution, where the size and frequency of patches adhere to specific power exponents, reflecting scale invariance and fractal structures within the system. However, as

external pressures intensify such as reduced precipitation or increased human interference, this power-law distribution can gradually be replaced by fragmented and random distributions. This shift serves as a significant indicator of system degradation (Fig. 9). For example, in dryland ecosystems in Africa and the Mediterranean, vegetation patterns that initially exhibited power-law distributions under sufficient precipitation and moderate grazing progressively disintegrate under the combined effects of reduced rainfall and overgrazing. Their spatial structure evolves into more irregular forms [53].

This transition from regular to irregular patterns and from power-law to fragmented distributions underscores the critical role of patch morphology in the process of system degradation. It not only reveals the underlying complexity of the internal dynamics of

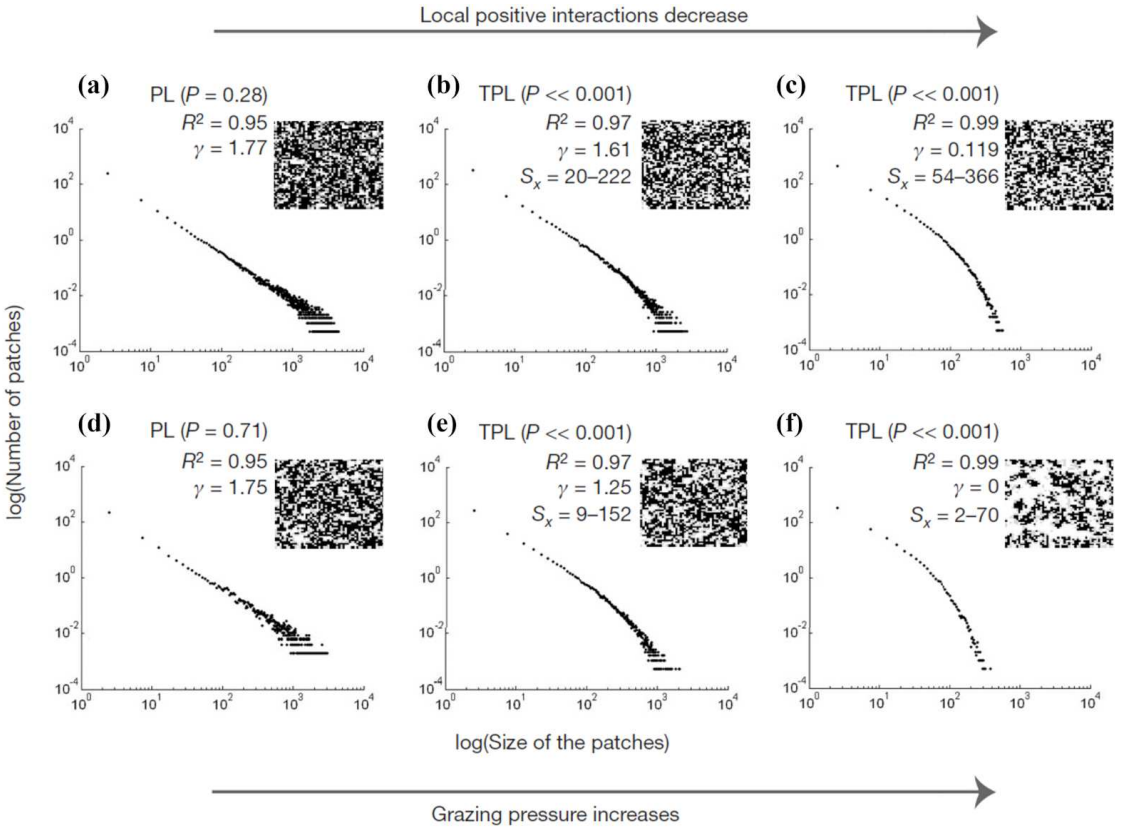

Figure 9: Patch-size distributions under varying levels of local positive interactions and grazing pressure, simulated using a stochastic cellular automaton model. (a), (d) Power-law (PL) distribution of patch sizes with a stable scaling exponent (γ) and non-significant P-values, reflecting minimal alteration in patch-size distribution when local positive interactions remain high or grazing pressure is low. (b), (c), (e), and (f) Transition to truncated power-law (TPL) distributions as local positive interactions decrease or grazing pressure intensifies. These changes are characterized by significant P-values, altered scaling exponents (γ), and truncation scales (S_x), indicating increased constraints on large patch formation. Insets: Spatial configurations of patches corresponding to each scenario. As interactions weaken or grazing pressure increases, patch structures become more fragmented and exhibit reduced connectivity. Source: Adapted from [53].

system but also provides an important early warning signal for ecosystem management. By monitoring changes in vegetation pattern morphology, particularly the progression of power-law distributions, it is possible to identify signs that the system is approaching a critical threshold, enabling timely interventions supported by scientific evidence.

3.1.3 Critical slowing down as an indicator

Critical slowing down is a key phenomenon in the dynamic evolution of vegetation systems and has become a research focus in recent years. Through systematic observations and model analyses, researchers have found that this phenomenon is closely related to ecosystem behavior near bifurcation points. When ecosystems approach bifurcation points, recovery times from disturbances increase significantly, while recovery rates slow dramatically. This phenomenon is reflected in both time-series and spatial pattern analyses. Dakos *et al.* [23] analyzed climate change time series and discovered that the recovery time of a system significantly increases as it approaches a critical threshold. The underlying principle of this phenomenon is that, as a system nears a bifurcation point, the strength of feedback mechanisms weakens, making it more difficult for the system to recover quickly from disturbances. This study laid the theoretical foundation for subsequent research focusing on critical slowing down as a core concept for ecological early-warning signals. As the theory incorporates concepts from spatial ecology, it propose that changes in spatial autocorrelation and spatial variance could also serve as early-warning indicators (Fig. 10). Through simulations and field data, Dakos *et al.* [22] verified that changes in spatial patterns could provide early cues of a critical state of system. For example, when ecosystems approach collapse, spatial autocorrelation between patches increases, and variance rises, reflecting a decline in the resilience.

Kéfi *et al.* [52] further advanced this field by studying vegetation patterns in arid ecosystems and identifying various spatial metrics to quantify critical slowing down, including spatial variance, autocorrelation, and the fragmentation and complexity of patterns (Table 2). Their research demonstrated that these spatial characteristics exhibit highly consistent trends during ecosystem degradation. Notably, increases in spatial variance have been shown to be key signals of a system nearing a critical threshold. This achievement provides new tools for monitoring ecosystem health through spatial patterns. Van Belzen *et al.* [115] through field studies on tidal marsh ecosystems, validated the extension of recovery time as a significant indicator of critical slowing down. Their results showed that the recovery time of a system significantly extended under increasing pressure, proving to be even more sensitive than traditional indicators like changes in spatial autocorrelation and variance. Such research further broadens the applicability of critical slowing down, making it a reliable method for quantifying ecosystem vulnerability. In addition, Forzieri *et al.* [32] provided global-scale evidence of critical slowing down in forest ecosystems under intensifying pressures from climate change. Using satellite data and temporal autocorrelation (TAC) as a core metric, their research revealed that declining resilience in tropical, temperate, and arid forests was strongly associated with an increase in TAC, a hallmark of critical slowing down. This rise in TAC indicates

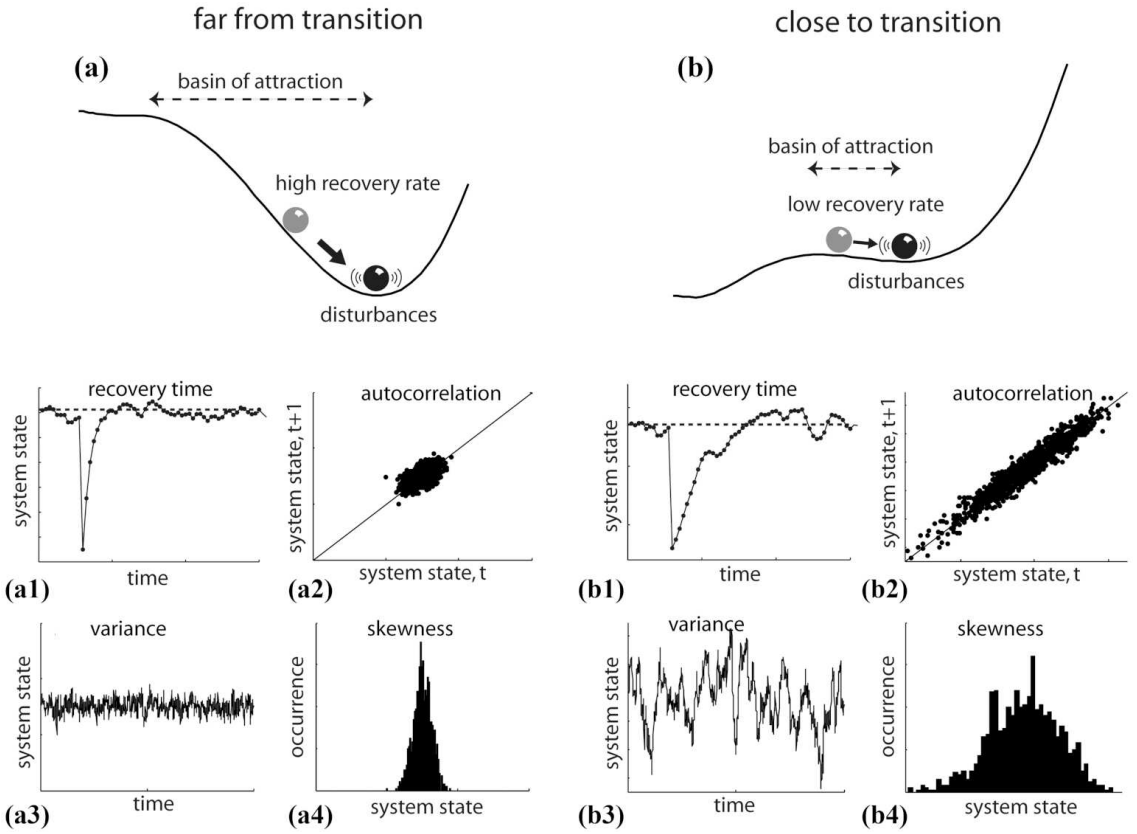

Figure 10: Conceptual representation of ecosystem resilience dynamics and critical slowing down indicators as the system approaches a transition. (a) System dynamics far from a critical transition, with a wide and deep basin of attraction. Effects from disturbances are quickly recovered, leading to a high recovery rate (a1). Autocorrelation remains low (a2), variance in system state is minimal (a3), and skewness is symmetrical (a4). (b) System dynamics close to a critical transition, with a narrowed and shallow basin of attraction. Disturbances take longer to recover, indicating a low recovery rate (b1). Autocorrelation increases as the system state becomes more predictable (b2), variance grows (b3), skewness shifts (b4). Source: Adapted from [22].

that forest systems are taking longer to recover from perturbations, reflecting a progressive loss of resilience. Their findings suggest that critical slowing down is a universal phenomenon, observable even in large-scale ecosystems through remotely sensed data.

Although traditional indicators such as spatial variance and autocorrelation have proven effective in quantifying critical slowing down, they exhibit limitations in capturing subtle changes in long-range spatial structures. Recently, spatial hyperuniformity has been proposed as a novel critical slowing down indicator, providing a new mathematical tool for uncovering key system dynamics by quantifying the scale-dependence of spatial density fluctuations [33, 48]. Hyperuniformity characterizes the long-range properties of density fluctuations in a system, with its core concept being to quantify the aggregation or dispersion of spatial distributions through the scaling law of density fluctuations with

Table 2: Traditional early warning signals of transitions in spatial data.

Indicator	Description	Formula	Refs.
Spatial correlation (Moran's I)	Measures the similarity between neighboring states, which increases as the system approaches a critical point.	$I=\frac{MN\sum w[i,j;m,n](z[i,j]-\bar{z})(z[m,n]-\bar{z})}{W\sum(z[m,n]-\bar{z})^2}$, $\bar{z}=\sum_{n=1}^{N}\sum_{m=1}^{M}\frac{z[m,n]}{MN}$.	[22], [24], [52]
Spatial variance	Indicates increased fluctuations as the system nears a critical transition.	$\sigma^2=\frac{1}{MN}\sum_{n=1}^{N}\sum_{m=1}^{M}(z[m,n]-\bar{z})^2$.	[22], [39], [52]
Spatial skewness	Reflects asymmetry in fluctuations, which may increase as the system approaches a critical point.	$\gamma=\frac{1}{MN}\sum_{n=1}^{N}\sum_{m=1}^{M}\frac{(z[m,n]-\bar{z})^3}{\sigma^3}$.	[22], [39]
Discrete Fourier transform (DET)	Transforms spatial patterns into frequency domain to evaluate fluctuation scales and periodicity.	$\hat{z}[p,q]=\frac{1}{MN}\sum_{m=0}^{M-1}\sum_{n=0}^{N-1}(z[m,n]-\bar{z})\times e^{-i2\pi(mp/M+nq/N)}$ $=\sum_{m=0}^{M-1}\sum_{n=0}^{N-1}(z[m,n]-\bar{z})\times(\cos(2\pi(mp/M+nq/N))-i\sin(2\pi(mp/M+nq/N)))$ $=a[p,q]-ib[p,q]$.	[52]
Power spectrum (2D-periodogram)	Describes a shift toward dominance of longer wavelengths in the power spectrum, reflecting increased memory effects.	$I[a,b]=MN(a[p,q]^2+b[p,q]^2)$.	[26], [52]
Patch-size distributions	Examines shifts in patch size distribution from power-law to other forms (e.g. exponential distribution) during system degradation.	$p(x)=\frac{\alpha-1}{x_{\min}}\left(\frac{x}{x_{\min}}\right)^{-\alpha}$, $PLR=1-\frac{\log_{10}(x_{\min})-\log_{10}(x_{\text{smallest}})}{\log_{10}(x_{\max})-\log_{10}(x_{\text{smallest}})}$.	[9], [51], [53]

scale. Its mathematical expression is given by [33, 111, 112]

$$\sigma^2\big(Q(S)\big)\sim S^{-b},$$

where $Q(S)$ represents the density distribution at scale S, σ^2 is the normalized variance, and b is the density fluctuation exponent, which measures the degree of fluctuation. In D-dimensional Euclidean space, the density fluctuation exponent b ranges within

$[0, D+1]$. When $D<b<D+1$, the system is defined as hyperuniform. Otherwise, the system is non-hyperuniform. In ecological systems, the density fluctuation exponent b can be further decomposed into short-range fluctuation exponent b_{sr} and long-range fluctuation exponent b_{lr}, which describe fluctuation characteristics at local and long-range scales, respectively. Among them, the long-range fluctuation index b_{lr} serves as a key indicator for identifying whether the system exhibits hyperuniformity, effectively capturing large-scale spatial organization and resource optimization capacity [33].

Moreover, Tirabassi and Masoller [110] introduced permutation entropy (PE) as a novel indicator with distinctive advantages. PE quantifies the complexity of system configurations across different spatial patterns, thereby capturing dynamic changes in vegetation structures as they approach critical thresholds. Tirabassi and Masoller *et al.* [110] showed that PE often exhibits non-monotonic behavior near critical transitions, typically reaching extreme values (either maxima or minima) before sharply declining. This behavior marks a crucial shift from high-biomass states to degraded states, offering an alternative perspective for early-warning signals. They further demonstrated that high-resolution data can reveal localized pattern adjustments, while low-resolution data yield smoother trends that help reduce false alarms. When combined with traditional metrics such as spatial variance and autocorrelation, PE enables a more comprehensive characterization of critical slowing down in ecosystems. For example, extreme values of PE may indicate bifurcation dynamics, whereas increased spatial variance reflects reduced ecosystem resilience. This multidimensional approach not only enhances the robustness of early-warning systems but also provides valuable guidance for monitoring ecological degradation and designing effective mitigation strategies.

Hyperuniformity and permutation entropy provide distinct dynamic perspectives for critical slowing down, expanding the research scope of critical slowing down. Hyperuniformity focuses on the optimization of ecosystems at broader spatial scales, while PE captures the intricate adjustment processes occurring at local scales. The integration of these two metrics enables a comprehensive multi-scale depiction of the critical dynamics in ecosystems, offering a robust theoretical foundation and technical tools for designing scientific intervention strategies and predicting ecosystem changes. In summary, the observation of critical slowing down offers strong scientific support for the early warning of ecosystem degradation.

3.2 Vegetation restoration and pattern reconstruction

Vegetation patterns are not only spatial representations of ecosystem states but also play a critical role in the natural restoration and reconstruction of degraded ecosystems. Studies show that the formation and reconstruction of these patterns are driven by intrinsic positive and negative feedback mechanisms while being significantly influenced by external interventions. By understanding and leveraging these mechanisms, scientists can design targeted restoration strategies, such as introducing spatially periodic forcing or regulatory methods based on optimal control theory, to maximize the efficiency and

long-term stability of ecosystem recovery. This section focuses on the role of human intervention strategies in pattern reconstruction, combining theoretical and empirical research to explore their potential applications.

3.2.1 Spatial periodic forcing

Spatial periodic forcing is an ecological restoration technique that stabilizes and guides the structure of vegetation patterns, optimizing water resource utilization and ecosystem functionality. Research demonstrates that periodic forcing can adjust the wavenumber and strength of the system, thereby influencing the stability and evolution of ecosystem patterns [71, 72]. This technique is particularly promising in arid and semi-arid regions where water resources are limited. The theoretical basis for periodic forcing can be described by a forced Swift-Hohenberg equation [71]

$$\partial_t u = \epsilon u - \left(\nabla^2 + k_0^2\right)^2 u - u^3 + \gamma u \cos(k_f x),$$

where u represents state variable, the parameter ϵ controls the distance from the instability threshold for pattern formation, k_0 is the natural wavenumber of the unforced system. The term $\gamma u \cos(k_f x)$ represents the spatial periodic forcing, where γ is the forcing amplitude and k_f is the forcing wavenumber, defining the strength and spatial periodicity of the external modulation, respectively. This periodic forcing interacts with the intrinsic dynamics of the system, introducing an external periodicity that stabilizes specific patterns by locking the natural wavenumber k_0 to the imposed wavenumber k_f or its harmonics, thereby transitioning the system to stable, regular states under appropriate conditions.

In one-dimensional systems, the approximate solution for stripe patterns can be expressed as

$$u \approx A \exp(ikx) + c.c.,$$

where the wavenumber k satisfies $k = k_f/n, n = 1,2,\ldots$, representing integer multiples of resonance. Periodic forcing stabilizes stripe patterns through the "wavenumber locking" mechanism. Specifically, the wavenumber of stripe patterns can be locked to a fraction of the forcing wavenumber (e.g. $k = k_f$, $k = k_f/2$), forming a "resonance tongue" region (Fig. 11(a)). In two-dimensional space, periodic forcing can induce other patterns. Unlike the one-dimensional stripe pattern ($\exp(ikx)$), two-dimensional systems can generate two-dimensional resonant patterns through the growth of oblique modes. The oblique modes are determined by the following relation:

$$\exp(i\mathbf{k}_\pm \cdot \mathbf{x}), \quad \mathbf{k}_\pm = \mathbf{k}_x \pm \mathbf{k}_y,$$

where $k_x = k_f/2, k_y = \sqrt{k_0^2 - k_x^2}$. These two-dimensional patterns have a wide range of existence along the forcing wavenumber k_f, but the upper limit is constrained by the 2:1 resonance of the stripe pattern, i.e. $0 < k_f < 2k_0$, because when $k_f = 2k_0$, the component k_x reaches its maximum possible value k_0. Fig. 11(b) illustrates the existence regions of

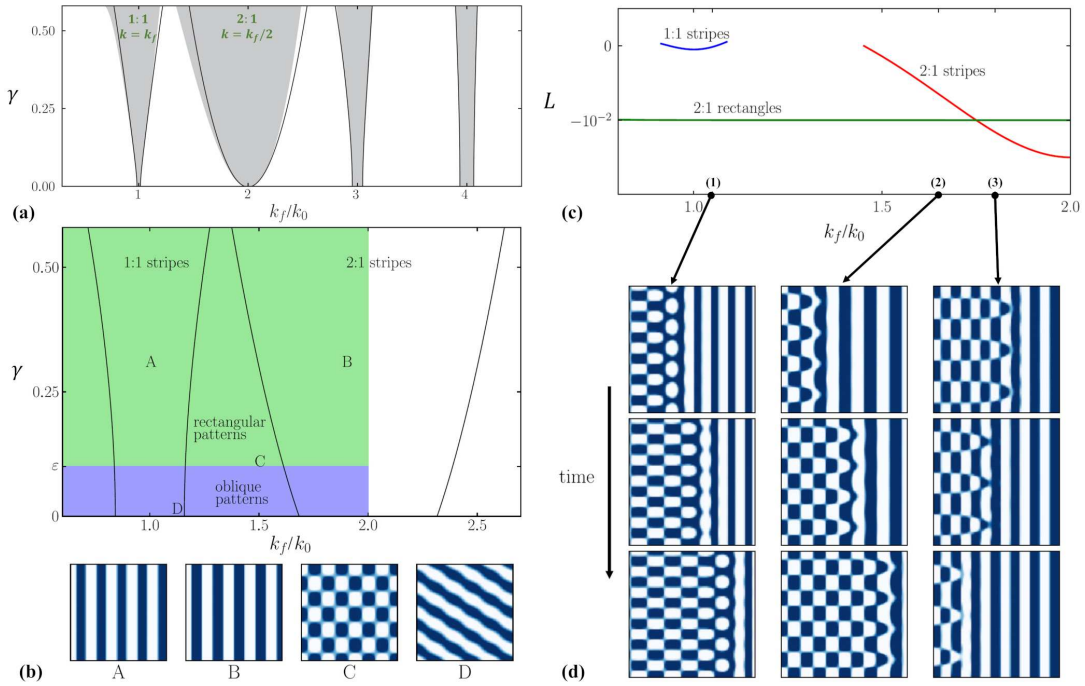

Figure 11: (a) The existence regions of n:1 resonances ($n=1,2,3,4$) as a function of forcing wavenumber ratio k_f/k_0 and forcing amplitude γ, highlighting resonant bands such as 1:1 stripes ($k=k_f$) and 2:1 stripes ($k=k_f/2$). (b) Classification of emergent patterns in the parameter plane $(k_f/k_0,\gamma)$, including 1:1 stripes (region A), 2:1 stripes (region B), rectangular patterns (region C), and oblique patterns (region D), with representative spatial structures shown below. (c) Energy (Lyapunov) analysis of pattern competition among 1:1 stripe patterns, 2:1 stripe patterns, and 2:1 rectangular patterns. (d) Time evolution of spatial patterns corresponding to parameter points (1), (2), and (3) in panel (c). (1) the competition between 1:1 stripes and 2:1 rectangular patterns; (2)(3) the competition between 2:1 stripes and 2:1 rectangular patterns. Source: Adapted from [71].

resonant rectangular and oblique patterns. Obviously, there is a overlap between the resonance regions of rectangular, oblique patterns, 1:1 and 2:1 stripe patterns. This overlap phenomenon indicates that different types of patterns will influence each other within a specific range of forcing parameters. For example, the system may experience complex phenomena such as pattern competition and conversion, which can affect the stability and dominance of patterns. To further determine which pattern is more advantageous within this bistable range, Mau *et al.* [71] introduced an energy (Lyapunov) functional

$$L=\int dr\left(-\frac{1}{2}[\epsilon+\gamma\cos(k_f x)]u^2+\frac{1}{4}u^4+\frac{1}{2}(\nabla^2 u+k_0^2 u^2)\right).$$

By calculating the values of this functional for different patterns (e.g. stripe, rectangular, and oblique), it is possible to quantify which pattern will dominate in competition based on the principle that lower energy corresponds to greater stability. The research shows that for 1:1 resonant stripe and rectangular patterns, the energy level directly determines their dominance. Rectangular patterns with lower energy tend to displace 1:1 stripe pat-

terns, occupying a larger spatial extent. In the 2 : 1 resonance range, the dominance of patterns changes with k_f/k_0 (Figs. 11(c), 11(d)). This change reflects the complex interactions between patterns, providing significant insights into the mechanisms of pattern formation and their control, and offering theoretical foundations for the effects of spatial forcing in restoration ecology. This theory has been applied to vegetation models, not only verifying its applicability but also revealing the performance and applicability of stripe and rhombic patterns in practical vegetation restoration [72,129].

3.2.2 Optimal control theory

Optimal control theory, as an advanced ecological management tool, has been widely applied to the design and optimization of ecosystem restoration strategies, particularly in the dynamic regulation of vegetation patterns [43,45,47,62]. The primary objective of optimal control theory is to maximize ecosystem recovery or functional optimization by adjusting external interventions (e.g. planting, irrigation, and terrain modification) within certain constraints. Its mathematical foundation combines dynamical systems with optimization theory, typically focusing on state variables and control variables to determine the optimal path that satisfies ecological goals. The dynamics of vegetation patterns in ecosystems can be represented by a reaction-diffusion model, generally expressed as

$$\frac{\partial u}{\partial t} = f(u,v,\nabla u) + D\nabla^2 u + c(x,t),$$

where $u(x,t)$ is the state variable representing vegetation density, $v(x,t)$ denotes environmental parameters, D is the diffusion coefficient that describes the spatial spreading capability of vegetation, $f(u,v,\nabla u)$ is a local nonlinear dynamical function reflecting growth, mortality, and competition mechanisms, and $c(x,t)$ is the control variable representing external interventions. In ecosystem restoration, optimal control theory provides a systematic approach by designing effective external intervention strategies to maximize ecological benefits while minimizing intervention costs. The control objective is typically formulated as an optimization problem, with the objective functional expressed as

$$J = \int_0^T \int_\Omega \left[g\big(u(x,t)\big) - \frac{\lambda}{2} c(x,t)^2 \right] dxdt,$$

where $g(u(x,t))$ is the benefit function representing the health of the ecosystem, λ is a weighting parameter balancing the cost of intervention and ecological benefits, and Ω represents the spatial domain. By optimizing J, the optimal control $c^*(x,t)$ can be determined, enabling efficient and sustainable ecosystem recovery.

Numerous studies on vegetation patterns have demonstrated that as precipitation levels change, ecosystems undergo a series of phase transitions, progressing from uniform coverage to gap patterns, labyrinth patterns, spotted patterns, and eventually degrading into bare-soil state [77]. Under low precipitation conditions, the natural recovery capacity of ecosystems is limited, necessitating the use of optimal control strategies for external intervention to reconstruct vegetation patterns. These interventions aim to utilize

human activities, such as targeted planting or localized water resource management, to effectively restore pattern structures under resource-scarce conditions. Here, we take the generalized Klausmeier model with cross diffusion as an example to demonstrate how to achieve pattern structure reconstruction by controlling human activities. The central task in this the optimal control problem lies in the formulation of the objective functional, which aims to steer the system toward desired spatial patterns while minimizing control costs. Specifically, it measures the deviation of state variables (e.g. vegetation and water) from target distributions and penalizes excessive interventions. The objective functional is given by

$$\begin{aligned} &O[n,w,u,b_n,b_w] \\ &=\frac{\kappa_1}{2}\int_\Omega [n(x,T)-n_{\text{tar}}(x,T)]^2dx+\frac{\kappa_2}{2}\int_\Omega [w(x,T)-w_{\text{tar}}(x,T)]^2dx \\ &\quad+\frac{\kappa_3}{2}\int_0^T\int_\omega u(x,t)^2dxdt+\frac{\kappa_4}{2}\int_0^T\int_{\partial\Omega} b_n(x,t)^2dsdt+\frac{\kappa_5}{2}\int_0^T\int_{\partial\Omega} b_w(x,t)^2dsdt, \end{aligned} \tag{3.1}$$

where $\kappa_i>0$ $(i=1,2,\ldots,5)$ are weight coefficients balancing the achievement of target patterns and intervention costs; n_{tar} and w_{tar} represent the target vegetation and water patterns, respectively; and u,b_n,b_w are control variables representing human activities within the region and on the boundaries. By minimizing O ($\min O$), the optimal control variables $u^*(x,t),b_n^*(x,t),b_w^*(x,t)$ can be obtained to achieve the dynamic restoration of the ecosystem. The dynamics of state variables $n(x,t)$ and $w(x,t)$ are governed by the following reaction-diffusion model:

$$\begin{cases} \dfrac{\partial n}{\partial t}=\Delta n+wn^2-\sigma n+\chi_\omega u & \text{in } \Omega_T=\Omega\times(0,T), \\ \dfrac{\partial w}{\partial t}=\mu\Delta w-\mu\delta\Delta n+a-w-wn^2 & \text{in } \Omega_T, \\ \dfrac{\partial n}{\partial \nu}+\alpha_1 n=b_n,\quad \mu\dfrac{\partial w}{\partial \nu}-\mu\delta\dfrac{\partial n}{\partial \nu}+\alpha_2 w=b_w & \text{in } \Sigma_T=\partial\Omega\times(0,T), \\ n(x,0)=\phi(x)\geq 0,\quad w(x,0)=\psi(x)\geq 0 & \text{in } \Omega, \end{cases} \tag{3.2}$$

where the initial conditions $(n(x,0),w(x,0))=(\phi(x),\psi(x))$ ensure a reasonable starting state. The characteristic function χ_ω identifies the intervention area ω, defined as

$$\chi_\omega=\begin{cases} 1, & x\in\omega, \\ 0, & x\notin\omega. \end{cases}$$

The selection of the control region ω is critical for the implementation of restoration strategies. When $\omega=\Omega$, control measures cover the entire region, achieving global intervention suitable for scenarios with abundant resources and widespread ecological degradation. Conversely, when $\omega\subset\Omega$, control measures are concentrated in specific areas,

aiming to efficiently allocate limited resources to prioritize the recovery of key degraded areas while inducing cascading effects on the broader ecosystem dynamics.

Research has shown that the proportion and number of the local control region significantly influence global ecosystem dynamics and the restoration of target patterns [43]. When the number of local control areas (ω) is consistent but have a small proportion, the control effect is mainly limited to the local area where the control is applied, and the matching degree between the global (Ω) vegetation distribution and the target state is not high. This indicates that small-scale local control can improve the ecological state of specific areas but has limited impact on the uncontrolled regions, making it insufficient for effective global pattern reconstruction. As the proportion of local control regions increases, cascading effects on the global dynamics become stronger. The expansion of the control area not only facilitates vegetation recovery within the controlled area but also induces significant effects in the uncontrolled regions, driving them toward the target patterns. When the control region reaches an appropriate proportion, it becomes possible to effectively establish target patterns across the entire region, significantly enhancing the overall efficiency of ecological restoration. This cascading effect demonstrates that moderately increasing the proportion of the control region can trigger positive feedback mechanisms in uncontrolled areas, driving comprehensive ecosystem recovery. Furthermore, when the proportion of the control region is held constant, the number of local control regions also plays a significant role. Studies have found that more dispersed control regions (i.e. there are more control areas) are more effective at promoting global pattern reconstruction. This is because dispersed control covers a wider spatial range, applying influence from multiple directions to the uncontrolled regions, thereby accelerating the restoration of vegetation patterns across the ecosystem.

However, regardless of increasing the proportion of the control region or optimizing their number, once these areas reach a certain threshold, further increases have a diminishing impact on overall improvement, eventually leading to saturation (Fig. 12). These results show that excessive control inputs do not significantly enhance restoration outcomes and may lead to resource wastage. Therefore, in practical applications, the proportion and number of control regions must be carefully planned based on the specific needs and resource conditions of the ecosystem to achieve an optimal balance between intervention costs and restoration benefits. The study of local control not only provides new theoretical foundations for optimizing ecological restoration strategies but also further validates the applicability of optimal control theory in managing complex ecosystems [43]. By carefully designing the proportion and distribution of control regions, it is possible to maximize global ecological restoration outcomes under resource-limited conditions, thereby achieving effective vegetation pattern reconstruction and long-term ecosystem stability.

Additionally, we have systematically explored other control strategies and summarized various methods, including terminal control, process control, and sparse control [45]. We have analyzed their applications and advantages in the dynamic regulation of vegetation patterns. Terminal control aims to steer the system toward a prescribed tar-

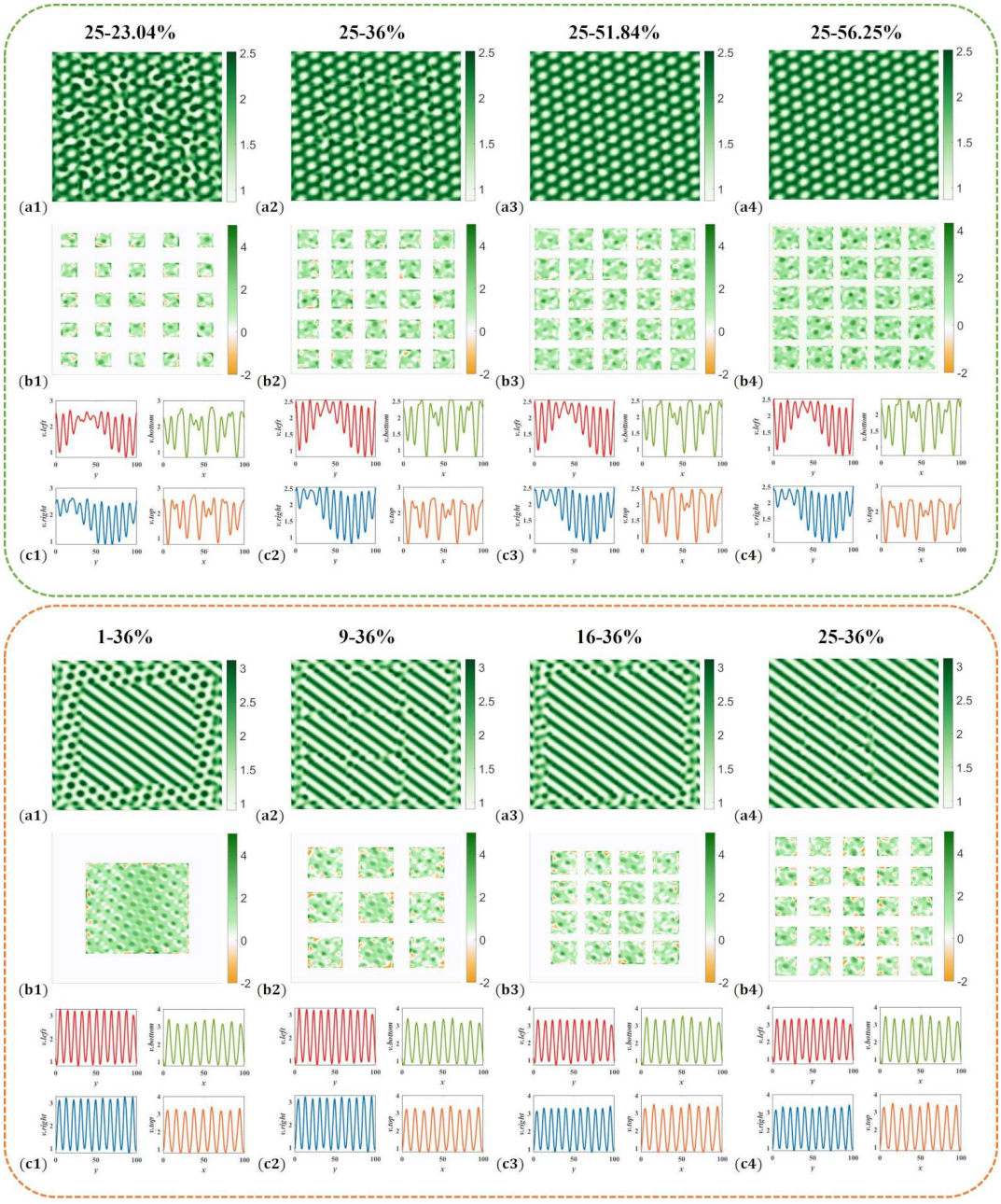

Figure 12: Top panel with green outline: Control area configurations with a fixed number of regions (25) and increasing proportions of the total area covered: 23.04%, 36%, 51.84%, 56.25%. Bottom panel with orange outline: Control area configurations with a fixed proportion (36% of the total area) and increasing numbers of control regions: 1,9,16, and 25. (a1)-(a4) Vegetation distribution after applying local control strategies, with the number of control areas and the total proportion of the controlled region indicated at the top of each column. (b1)-(b4) Distribution of control variable intensities corresponding to each configuration. (c1)-(c4) Boundary control distribution for the four boundaries (top, bottom, left, and right), with each color-coded plot representing one boundary. Source: Adapted from [43].

get state at the final time by appropriately adjusting the control variables throughout the control horizon [47]. In contrast, process control emphasizes optimizing the performance of system over the entire time horizon. Both methods have demonstrated effective outcomes in restoring arid ecosystems but often require higher intervention costs. Sparse control, as a resource-saving strategy, introduces L^1-norm regularization to limit the number of non-zero control inputs, significantly reducing intervention costs. This approach achieves substantial cost savings while maintaining effective ecological restoration. By combining these methods, we validated the theoretical and practical applicability of optimal control strategies across multiple vegetation models. In summary, various optimal control strategies possess distinct advantages, making them suitable for different ecological restoration needs. Terminal control is ideal for systems with clearly defined targets, while process control ensures dynamic regulation over time. Sparse control achieves effective interventions with reduced resource input, and local and boundary control maximize resource utilization through spatial selectivity. In practical applications, selecting and combining these strategies based on the specific needs and constraints of the ecosystem allows for efficient ecological restoration and provides a solid scientific foundation for managing complex ecosystems.

4 Summary and outlook

Vegetation patterns are important manifestations of the complex dynamics of ecosystems, reflecting the stability and resilience of systems in resource allocation, environmental pressures, and self-organization processes [3, 5, 15, 17, 21, 57, 98]. This paper systematically reviews and summarizes relevant studies, exploring the mechanisms of vegetation pattern formation, early warning signals during degradation processes, and strategies for restoration and reconstruction. These studies highlight the unique advantages of vegetation patterns as spatial representations of ecosystem states and emphasize their theoretical and practical value in ecosystem management and restoration. Numerous studies have shown that vegetation patterns are driven by positive and negative feedback mechanisms and are influenced by environmental gradients, diffusion processes, and nonlinear dynamics [55, 69, 76, 77]. From regular patterns to irregular patterns, the evolution of vegetation patterns not only reflects the adaptability of ecosystem to environmental disturbances but also reveals its dynamic characteristics as it approaches critical thresholds. In recent years, traditional indicators such as spatial variance and autocorrelation have been widely used to quantify the phenomenon of critical slowing down in ecosystems, providing effective tools for early warning. However, these indicators face limitations in capturing long-range spatial dynamics. Emerging indicators such as hyperuniformity and permutation entropy have not only addressed these limitations but also broadened the scope of research into the critical dynamics of ecosystems [33, 79, 110]. These multi-scale, multi-dimensional studies have laid a solid foundation for accurately monitoring and predicting the critical behaviors of ecosystems.

The restoration and reconstruction of vegetation patterns are critical directions in ecosystem management. With the introduction of optimal control theory, researchers can design and optimize external intervention strategies to maximize ecosystem functionality under resource constraints. For instance, optimal control frameworks based on reaction-diffusion models can achieve targeted regulation of vegetation patterns by optimizing human activities [45,113]. While spatial periodic forcing and optimal control have been studied separately, their integration holds promise for improving restoration strategies. Combining spatial periodic forcing with objective functional optimization may offer a unified framework that not only strengthens the theoretical basis of ecosystem management but also provides effective tools for restoring degraded vegetation in arid and semi-arid regions.

Despite significant advances in the study of vegetation patterns, several unresolved challenges remain in both theory and application. At the modeling level, the complexity of system dynamics and the uncertainty of parameters pose difficulties for reliable predictions, and the diversity of ecosystems requires models with greater flexibility and adaptability in representing dynamic mechanisms. At the application level, parameter estimation is often constrained by sparse or noisy field data, scale mismatches arise between simplified model assumptions and heterogeneous natural conditions, and the scarcity of long-term, high-resolution monitoring data limits model calibration and validation, particularly in arid and semi-arid regions. Moreover, long-term projections remain uncertain, as climate variability, extreme events, and human interventions may drive ecosystems beyond the scope of current theoretical frameworks. Addressing these issues will require closer integration of modeling with remote sensing observations, data assimilation, and experimental studies, as well as the development of adaptive and data-driven frameworks. Future studies may also incorporate non-local interactions, topographical features, and climate change into control frameworks, and strengthen the linkage between local processes and global-scale ecosystem changes, thereby expanding the applicability of vegetation pattern models and providing more practical support for ecosystem management and restoration.

A particularly important direction is the development of multi-scale modeling frameworks that explicitly connect microscale processes, mesoscale patterns, and macroscale landscape functions. For example, root-soil interactions at the plant level determine local feedbacks in water and nutrient use [49, 108, 116], which aggregate into patch-level dynamics, while these in turn shape landscape-scale transitions such as desertification or regime shifts. Hierarchical and hybrid models provide promising tools to integrate these scales, enabling the translation of fine-scale mechanisms into predictions of large-scale ecosystem resilience and functionality. Such approaches are crucial for advancing both theoretical understanding and practical management of vegetation systems under climate and anthropogenic pressures.

Furthermore, as the impacts of climate change and human activities on ecosystems intensify, the significance of vegetation pattern research becomes increasingly prominent [11, 37, 50, 60–62, 103, 125]. Advanced remote sensing technologies and artificial

intelligence tools will play a central role in the collection, analysis, and modeling of ecological data, providing technical support for high-resolution ecosystem monitoring and prediction [2, 18]. Furthermore, interdisciplinary collaboration integrating mathematics, physics, computational science, and ecology holds promise for constructing a unified theoretical framework, comprehensively revealing the critical role of vegetation patterns in the dynamic regulation of ecosystems. In conclusion, research on vegetation patterns not only deepens our understanding of ecosystem resilience, stability, and complex dynamics but also provides vital scientific evidence for achieving global sustainable development goals.

Acknowledgments

This work is supported by the National Natural Science Foundation of China (Grant No. 42275034), by the Scientific Activities of Selected Returned Overseas Professionals in Shanxi Province (Grant No. 20230013), by the Distinguished Young Scholars Foundation of Shanxi Scientific Committee (Grant No. 202303021223009), by the Postgraduate Education Innovation Program of Shanxi Province (Grant No. 2024KY017), and by the China Scholarship Council.

References

[1] M. Alfaro, H. Izuhara, and M. Mimura, *On a nonlocal system for vegetation in drylands*, J. Math. Biol., 77:1761–1793, 2018.

[2] B. Ayhan, C. Kwan, B. Budavari, L. Kwan, Y. Lu, D. Perez, J. Li, D. Skarlatos, and M. Vlachos, *Vegetation detection using deep learning and conventional methods*, Remote Sens., 12:2502, 2020.

[3] R. Bastiaansen, A. Doelman, M. B. Eppinga, and M. Rietkerk, *The effect of climate change on the resilience of ecosystems with adaptive spatial pattern formation*, Ecol. Lett., 23:414–429, 2020.

[4] R. Bastiaansen, O. Jaïbi, V. Deblauwe, M. B. Eppinga, K. Siteur, E. Siero, S. Mermoz, A. Bouvet, A. Doelman, and M. Rietkerk, *Multistability of model and real dryland ecosystems through spatial self-organization*, Proc. Natl. Acad. Sci. USA, 115:11256–11261, 2018.

[5] S. Bathiany, D. Nian, M. Drüke, and N. Boers, *Resilience indicators for tropical rainforests in a dynamic vegetation model*, Glob. Change Biol., 30:e17613, 2024.

[6] M. Baudena and M. Rietkerk, *Complexity and coexistence in a simple spatial model for arid savanna ecosystems*, Theor. Ecol., 6:131–141, 2013.

[7] J. J. R. Bennett and J. A. Sherratt, *Long-distance seed dispersal affects the resilience of banded vegetation patterns in semi-deserts*, J. Math. Biol., 481:151–161, 2019.

[8] M. Berdugo, J. J. Gaitán, M. Delgado-Baquerizo, T. W. Crowther, and V. Dakos, *Prevalence and drivers of abrupt vegetation shifts in global drylands*, Proc. Natl. Acad. Sci. USA, 119:e2123393119, 2022.

[9] M. Berdugo, S. Kéfi, S. Soliveres, and F. T. Maestre, *Plant spatial patterns identify alternative ecosystem multifunctionality states in global drylands*, Nat. Ecol. Evol., 1:0003, 2017.

[10] P. N. Bernardino et al., *Predictability of abrupt shifts in dryland ecosystem functioning*, Nat. Clim. Change, 15:86–91, 2025.

[11] M. Bianchini et al., *Modeling climate-driven vegetation changes under contrasting temperate and arid conditions in the Mediterranean basin*, Ecol. Evol., 15:e70753, 2025.
[12] N. Boers and M. Rypdal, *Critical slowing down suggests that the western Greenland ice sheet is close to a tipping point*, Proc. Natl. Acad. Sci. USA, 118:e2024192118, 2021.
[13] F. Borgogno, P. D'odorico, F. Laio, and L. Ridolfi, *Mathematical models of vegetation pattern formation in ecohydrology*, Rev. Geophys., 47:RG000256, 2009.
[14] T. M. Bury, R. Sujith, I. Pavithran, M. Scheffer, T. M. Lenton, M. Anand, and C. T. Bauch, *Deep learning for early warning signals of tipping points*, Proc. Natl. Acad. Sci. USA, 118:e2106140118, 2021.
[15] J. E. Buxton, J. F. Abrams, C. A. Boulton, N. Barlow, C. Rangel Smith, S. Van Stroud, K. J. Lees, and T. M. Lenton, *Quantitatively monitoring the resilience of patterned vegetation in the Sahel*, Glob. Change Biol., 28:571–587, 2022.
[16] S. R. Carpenter and W. A. Brock, *Rising variance: A leading indicator of ecological transition*, Ecol. Lett., 9:311–318, 2006.
[17] Z. Chen, P. Fan, X. Hou, F. Ji, L. Li, Z. Qian, G. Feng, and G. Sun, *Analysis of global vegetation resilience under different future climate scenarios*, Clim. Dyn., 62:7967–7980, 2024.
[18] Z. Chen, H. Liu, C. Xu, X. Wu, B. Liang, J. Cao, and D. Chen, *Modeling vegetation greenness and its climate sensitivity with deep-learning technology*, Ecol. Evol., 11:7335–7345, 2021.
[19] Z. Chen, J. Liu, L. Li, Y. Wu, G. Feng, Z. Qian, and G.-Q. Sun, *Effects of climate change on vegetation patterns in Hulun Buir Grassland*, Phys. A, 597:127275, 2022.
[20] Z. Chen, Y.-P. Wu, G.-L. Feng, Z.-H. Qian, and G.-Q. Sun, *Effects of global warming on pattern dynamics of vegetation: Wuwei in China as a case*, Appl. Math. Comput., 390:125666, 2021.
[21] C. Ciemer, N. Boers, M. Hirota, J. Kurths, F. Müller-Hansen, R. S. Oliveira, and R. Winkelmann, *Higher resilience to climatic disturbances in tropical vegetation exposed to more variable rainfall*, Nat. Geosci., 12:174–179, 2019.
[22] V. Dakos, S. Kéfi, M. Rietkerk, E. H. van Nes, and M. Scheffer, *Slowing down in spatially patterned ecosystems at the brink of collapse*, Am. Nat., 177:E153–E166, 2011.
[23] V. Dakos, M. Scheffer, E. H. van Nes, V. Brovkin, V. Petoukhov, and H. Held, *Slowing down as an early warning signal for abrupt climate change*, Proc. Natl. Acad. Sci. USA, 105:14308–14312, 2008.
[24] V. Dakos, E. H. van Nes, R. Donangelo, H. Fort, and M. Scheffer, *Spatial correlation as leading indicator of catastrophic shifts*, Theor. Ecol., 3:163–174, 2010.
[25] H. de Paoli, T. van der Heide, A. van den Berg, B. R. Silliman, P. M. J. Herman, and J. van de Koppel, *Behavioral self-organization underlies the resilience of a coastal ecosystem*, Proc. Natl. Acad. Sci. USA, 114:8035–8040, 2017.
[26] V. Deblauwe, P. Couteron, O. Lejeune, J. Bogaert, and N. Barbier, *Environmental modulation of self-organized periodic vegetation patterns in Sudan*, Ecography, 34:990–1001, 2011.
[27] L. Eigentler and J. A. Sherratt, *Analysis of a model for banded vegetation patterns in semi-arid environments with nonlocal dispersal*, J. Math. Biol., 77:739–763, 2018.
[28] L. Eigentler and J. A. Sherratt, *Long-range seed dispersal enables almost stationary patterns in a model for dryland vegetation*, J. Math. Biol., 86:15, 2023.
[29] M. A. Ferré, I. Pavithran, B. K. Bera, H. Uecker, and E. Meron, *Vegetation pattern formation and community assembly under drying climate trends*, Chaos, 35:093114, 2025.
[30] U. Feudel, A. N. Pisarchik, and K. Showalter, *Multistability and tipping: From mathematics and physics to climate and brain – Minireview and preface to the focus issue*, Chaos, 28:033501, 2018.
[31] B. M. Flores et al., *Critical transitions in the Amazon forest system*, Nature, 626:555–564, 2024.

[32] G. Forzieri, V. Dakos, N. G. McDowell, A. Ramdane, and A. Cescatti, *Emerging signals of declining forest resilience under climate change*, Nature, 608:534–539, 2022.
[33] Z. Ge, *The hidden order of Turing patterns in arid and semi-arid vegetation ecosystems*, Proc. Natl. Acad. Sci. USA, 120:e2306514120, 2023.
[34] S. Getzin et al., *Discovery of fairy circles in Australia supports self-organization theory*, Proc. Natl. Acad. Sci. USA, 113:3551–3556, 2016.
[35] E. Gilad, J. von Hardenberg, A. Provenzale, M. Shachak, and E. Meron, *Ecosystem engineers: From pattern formation to habitat creation*, Phys. Rev. Lett., 93:098105, 2004.
[36] E. Gilad, J. von Hardenberg, A. Provenzale, M. Shachak, and E. Meron, *A mathematical model of plants as ecosystem engineers*, J. Theor. Biol., 244:680–691, 2007.
[37] P. Gonzalez, R. P. Neilson, J. M. Lenihan, and R. J. Drapek, *Global patterns in the vulnerability of ecosystems to vegetation shifts due to climate change*, Glob. Ecol. Biogeogr., 19:755–768, 2010.
[38] V. Guttal and C. Jayaprakash, *Changing skewness: An early warning signal of regime shifts in ecosystems*, Ecol. Lett., 11:450–460, 2008.
[39] V. Guttal and C. Jayaprakash, *Spatial variance and spatial skewness: Leading indicators of regime shifts in spatial ecological systems*, Theor. Ecol., 2:3–12, 2009.
[40] S. I. Higgins and S. Scheiter, *Atmospheric CO_2 forces abrupt vegetation shifts locally, but not globally*, Nature, 488:209–212, 2012.
[41] R. HilleRisLambers, M. Rietkerk, F. van den Bosch, H. H. T. Prins, and H. de Kroon, *Vegetation pattern formation in semi-arid grazing systems*, Ecology, 82:50–61, 2001.
[42] M. Hirota, M. Holmgren, E. H. van Nes, and M. Scheffer, *Global resilience of tropical forest and savanna to critical transitions*, Science, 334:232–235, 2011.
[43] L.-F. Hou, S.-P. Gao, L.-L. Chang, Y.-P. Wu, G.-L. Feng, Z. Wang, and G.-Q. Sun, *Vegetation restoration strategies in arid or semi-arid regions – From the perspective of optimal control*, Chaos, 34:113109, 2024.
[44] L.-F. Hou, S.-P. Gao, and G.-Q. Sun, *Two types of fairy circles coexist in a vegetation – water model*, Nonlinear Dyn., 111:7883–7898, 2023.
[45] L.-F. Hou, L. Li, L. Chang, Z. Wang, and G.-Q. Sun, *Pattern dynamics of vegetation based on optimal control theory*, Nonlinear Dyn., 113:1–23, 2025.
[46] L.-F. Hou, L. Li, R. Chen, Y.-P. Wu, G.-L. Feng, and G.-Q. Sun, *Vegetation dynamics: Modeling, mechanisms, and emergent properties*, Phys. Rep., 1145:1–87, 2025.
[47] L.-F. Hou, G.-Q. Sun, and M. Perc, *The impact of heterogeneous human activity on vegetation patterns in arid environments*, Commun. Nonlinear Sci. Numer. Simul., 126:107461, 2023.
[48] W. Hu, L. Cui, M. Delgado-Baquerizo, R. Solé, S. Kéfi, M. Berdugo, N. Xu, B. Wang, Q.-X. Liu, and C. Xu, *Causes and consequences of disordered hyperuniformity in global drylands*, Proc. Natl. Acad. Sci. USA, 122:e2504496122, 2025.
[49] Inderjit, R. M. Callaway, and E. Meron, *Belowground feedbacks as drivers of spatial self-organization and community assembly*, Phys. Life Rev., 38:1–24, 2021.
[50] L. Jiang, G. Jiapaer, A. Bao, H. Guo, and F. Ndayisaba, *Vegetation dynamics and responses to climate change and human activities in Central Asia*, Sci. Total Environ., 599:967–980, 2017.
[51] S. Kéfi, A. Génin, A. Garcia-Mayor, E. Guirado, J. S. Cabral, M. Berdugo, J. Guerber, R. Solé, and F. T. Maestre, *Self-organization as a mechanism of resilience in dryland ecosystems*, Proc. Natl. Acad. Sci. USA, 121:e2305153121, 2024.
[52] S. Kéfi, V. Guttal, W. A. Brock, S. R. Carpenter, A. M. Ellison, V. N. Livina, D. A. Seekell, M. Scheffer, E. H. van Nes, and V. Dakos, *Early warning signals of ecological transitions: Methods for spatial patterns*, PLoS ONE, 9:e92097, 2014.
[53] S. Kéfi, M. Rietkerk, C. Alados, Y. Pueyo, V. P. Papanastasis, A. ElAich, and P. C. de Ruiter,

Spatial vegetation patterns and imminent desertification in Mediterranean arid ecosystems, Nature, 449:213–217, 2007.

[54] S. Kefi, M. Rietkerk, and G. G. Katul, *Vegetation pattern shift as a result of rising atmospheric CO_2 in arid ecosystems*, Theor. Popul. Biol., 74:332–344, 2008.

[55] C. A. Klausmeier, *Regular and irregular patterns in semiarid vegetation*, Science, 284:1826–1828, 1999.

[56] C. Kuehn, *A mathematical framework for critical transitions: Normal forms, variance and applications*, J. Nonlinear Sci., 23:457–510, 2013.

[57] S. Lavorel, *Ecological diversity and resilience of mediterranean vegetation to disturbance*, Divers. Distrib., 5:3–13, 1999.

[58] R. Lefever and O. Lejeune, *On the origin of tiger bush*, Bull. Math. Biol., 59:263–294, 1997.

[59] J. Li, G.-Q. Sun, and Z. Jin, *Interactions of time delay and spatial diffusion induce the periodic oscillation of the vegetation system*, Discrete Contin. Dyn. Syst. Ser. B, 27:2147–2172, 2022.

[60] J. Li, G.-Q. Sun, L. Li, Z. Jin, and Y. Yuan, *The effect of grazing intensity on pattern dynamics of the vegetation system*, Chaos Solit. Fractals, 175:114025, 2023.

[61] L. Li, Y.-Z. Pang, G.-Q. Sun, and S. Ruan, *Impact of climate change on vegetation patterns in Altay Prefecture, China*, Math. Med. Biol., 41:53–80, 2024.

[62] J. Liang and G.-Q. Sun, *Effects of climate change on vegetation pattern in Baotou, China*, Nonlinear Dyn., 112:8675–8693, 2024.

[63] Y. Lin, G. Han, M. Zhao, and S. X. Chang, *Spatial vegetation patterns as early signs of desertification: A case study of a desert steppe in Inner Mongolia, China*, Landsc. Ecol., 25:1519–1527, 2010.

[64] Z. Liu, X. Zhang, X. Ru, T.-T. Gao, J. M. Moore, and G. Yan, *Early predictor for the onset of critical transitions in networked dynamical systems*, Phys. Rev. X., 14:031009, 2024.

[65] M. T. Löbmann, C. Geitner, C. Wellstein, and S. Zerbe, *The influence of herbaceous vegetation on slope stability – A review*, Earth-Sci. Rev., 209:103328, 2020.

[66] M. López Pereira, V. O. Sadras, W. Batista, J. J. Casal, and A. J. Hall, *Light-mediated self-organization of sunflower stands increases oil yield in the field*, Proc. Natl. Acad. Sci. USA, 114:7975–7980, 2017.

[67] S. Ma, J. Ren, C. Wu, and Q. He, *Extreme precipitation events trigger abrupt vegetation succession in emerging coastal wetlands*, Catena, 241:108066, 2024.

[68] F. T. Maestre and A. Escudero, *Is the patch size distribution of vegetation a suitable indicator of desertification processes?*, Ecology, 90:1729–1735, 2009.

[69] R. Martínez-García, J. M. Calabrese, E. Hernández-García, and C. López, *Vegetation pattern formation in semiarid systems without facilitative mechanisms*, Geophys. Res. Lett., 40:6143–6147, 2013.

[70] R. Martínez-García, J. M. Calabrese, and C. López, *Spatial patterns in mesic savannas: The local facilitation limit and the role of demographic stochasticity*, J. Theor. Biol., 333:156–165, 2013.

[71] Y. Mau, A. Hagberg, and E. Meron, *Spatial periodic forcing can displace patterns it is intended to control*, Phys. Rev. Lett., 109:034102, 2012.

[72] Y. Mau, L. Haim, and E. Meron, *Reversing desertification as a spatial resonance problem*, Phys. Rev. E, 91:012903, 2015.

[73] E. Meron, *Pattern-formation approach to modelling spatially extended ecosystems*, Ecol. Model., 234:70–82, 2012.

[74] E. Meron, *Pattern formation – A missing link in the study of ecosystem response to environmental changes*, Math Biosci., 271:1–18, 2016.

[75] E. Meron, *From patterns to function in living systems: Dryland ecosystems as a case study*, Annu.

Rev. Condens. Matter Phys., 9:79–103, 2018.
[76] E. Meron, *Vegetation pattern formation: The mechanisms behind the forms*, Phys. Today, 72:30–36, 2019.
[77] E. Meron, E. Gilad, J. Von Hardenberg, M. Shachak, and Y. Zarmi, *Vegetation patterns along a rainfall gradient*, Chaos Solit. Fractals, 19:367–376, 2004.
[78] W. Pałubicki, M. Makowski, W. Gajda, T. Hädrich, D. L. Michels, and S. Pirk, *Ecoclimates: Climate-response modeling of vegetation*, ACM Trans. Graph., 41:1–19, 2022.
[79] Y.-Z. Pang, L. Li, and Z. Jin, *Early warning signals of critical transitions in ecosystems: Entropy reduction in vegetation spatial patterns*, Nonlinear Dyn., 113:15597–15618, 2025.
[80] B. Pichon, I. Gounand, S. Donnet, and S. Kéfi, *The interplay of facilitation and competition drives the emergence of multistability in dryland plant communities*, Ecology, 105:e4369, 2024.
[81] Y. Pueyo, S. Kéfi, C. Alados, and M. Rietkerk, *Dispersal strategies and spatial organization of vegetation in arid ecosystems*, Oikos, 117:1522–1532, 2008.
[82] M. Reichstein, M. Bahn, M. D. Mahecha, J. Kattge, and D. D. Baldocchi, *Linking plant and ecosystem functional biogeography*, Proc. Natl. Acad. Sci. USA, 111:13697–13702, 2014.
[83] M. Rietkerk, R. Bastiaansen, S. Banerjee, J. van de Koppel, M. Baudena, and A. Doelman, *Evasion of tipping in complex systems through spatial pattern formation*, Science, 374:eabj0359, 2021.
[84] M. Rietkerk, M. C. Boerlijst, F. van Langevelde, R. HilleRisLambers, J. van de Koppel, L. Kumar, H. H. T. Prins, and A. M. de Roos, *Self-organization of vegetation in arid ecosystems*, Am. Nat., 160:524–530, 2002.
[85] M. Rietkerk, S. C. Dekker, P. C. de Ruiter, and J. van de Koppel, *Self-organized patchiness and catastrophic shifts in ecosystems*, Science, 305:1926–1929, 2004.
[86] M. Rietkerk and J. van de Koppel, *Regular pattern formation in real ecosystems*, Trends Ecol. Evol., 23:169–175, 2008.
[87] M. Scheffer, *Critical Transitions in Nature and Society*, in: Princeton Studies in Complexity, Vol. 16, Princeton University Press, 2020.
[88] M. Scheffer, J. Bascompte, W. A. Brock, V. Brovkin, S. R. Carpenter, V. Dakos, H. Held, E. H. van Nes, M. Rietkerk, and G. Sugihara, *Early-warning signals for critical transitions*, Nature, 461:53–59, 2009.
[89] M. Scheffer and S. R. Carpenter, *Catastrophic regime shifts in ecosystems: Linking theory to observation*, Trends Ecol. Evol., 18:648–656, 2003.
[90] M. Scheffer, S. Carpenter, J. A. Foley, C. Folke, and B. Walker, *Catastrophic shifts in ecosystems*, Nature, 413:591–596, 2001.
[91] M. Scheffer, S. R. Carpenter, T. M. Lenton, J. Bascompte, W. Brock, V. Dakos, J. van de Koppel, I. A. van de Leemput, S. A. Levin, E. H. van Nes, M. Pascual, and J. Vandermeer, *Anticipating critical transitions*, Science, 338:344–348, 2012.
[92] F. Schweisguth and F. Corson, *Self-organization in pattern formation*, Dev. Cell, 49:659–677, 2019.
[93] J. A. Sherratt, *An analysis of vegetation stripe formation in semi-arid landscapes*, J. Math. Biol., 51:183–197, 2005.
[94] J. A. Sherratt, *Pattern solutions of the Klausmeier model for banded vegetation in semi-arid environments I*, Nonlinearity, 23:2657, 2010.
[95] J. A. Sherratt, *Pattern solutions of the Klausmeier model for banded vegetation in semiarid environments IV: Slowly moving patterns and their stability*, SIAM J. Appl. Math., 73:330–350, 2013.
[96] J. A. Sherratt, *Pattern solutions of the Klausmeier model for banded vegetation in semiarid envi-*

ronments V: The transition from patterns to desert, SIAM J. Appl. Math., 73:1347–1367, 2013.
[97] J. A. Sherratt, *Using wavelength and slope to infer the historical origin of semiarid vegetation bands*, Proc. Natl. Acad. Sci. USA, 112:4202–4207, 2015.
[98] E. Siero, A. Doelman, M. B. Eppinga, J. D. M. Rademacher, M. Rietkerk, and K. Siteur, *Striped pattern selection by advective reaction-diffusion systems: Resilience of banded vegetation on slopes*, Chaos, 25:036411, 2015.
[99] T. Smith and N. Boers, *Global vegetation resilience linked to water availability and variability*, Nat. Commun., 14:498, 2023.
[100] T. Smith, D. Traxl, and N. Boers, *Empirical evidence for recent global shifts in vegetation resilience*, Nat. Clim. Change, 12:477–484, 2022.
[101] G.-Q. Sun, R. He, L.-F. Hou, X. Luo, S. Gao, L. Chang, Y. Wang, and Z.-K. Zhang, *Optimal control of spatial diseases spreading in networked reaction-diffusion systems*, Phys. Rep., 1111:1–64, 2025.
[102] G.-Q. Sun, L.-F. Hou, L. Li, Z. Jin, and H. Wang, *Spatial dynamics of a vegetation model with uptake – diffusion feedback in an arid environment*, J. Math. Biol., 85:50, 2022.
[103] G.-Q. Sun, L. Li, J. Li, C. Liu, Y.-P. Wu, S. Gao, Z. Wang, and G.-L. Feng, *Impacts of climate change on vegetation pattern: Mathematical modeling and data analysis*, Phys. Life Rev., 43:239–270, 2022.
[104] G.-Q. Sun, C.-H. Wang, L.-L. Chang, Y.-P. Wu, L. Li, and Z. Jin, *Effects of feedback regulation on vegetation patterns in semi-arid environments*, Appl. Math. Model., 61:200–215, 2018.
[105] G.-Q. Sun, Z.-C. Xue, L. Li, J. Li, C. I. del Genio, and S. Boccaletti, *Chimera states with multiple coexisting solutions*, Phys. Rev. Res., 7:023289, 2025.
[106] G.-Q. Sun, H.-T. Zhang, Y.-L. Song, L. Li, and Z. Jin, *Dynamic analysis of a plant-water model with spatial diffusion*, J. Differential Equations, 329:395–430, 2022.
[107] G.-Q. Sun, H.-T. Zhang, J.-S. Wang, J. Li, Y. Wang, L. Li, Y.-P. Wu, G.-L. Feng, and Z. Jin, *Mathematical modeling and mechanisms of pattern formation in ecological systems: A review*, Nonlinear Dyn., 104:1677–1696, 2021.
[108] M. P. Thakur, W. H. van der Putten, R. A. Wilschut, G. C. Veen, P. Kardol, J. van Ruijven, E. Allan, C. Roscher, M. van Kleunen, and T. M. Bezemer, *Plant-soil feedbacks and temporal dynamics of plant diversity-productivity relationships*, Trends Ecol. Evol., 36:651–661, 2021.
[109] C. Tian, Z. Ling, and L. Zhang, *Delay-driven spatial patterns in a network-organized semiarid vegetation model*, Appl. Math. Comput., 367:124778, 2020.
[110] G. Tirabassi and C. Masoller, *Entropy-based early detection of critical transitions in spatial vegetation fields*, Proc. Natl. Acad. Sci. USA, 120:e2215667120, 2023.
[111] S. Torquato, *Hyperuniform states of matter*, Phys. Rep., 745:1–95, 2018.
[112] S. Torquato and F. H. Stillinger, *Local density fluctuations, hyperuniformity, and order metrics*, Phys. Rev. E, 68:041113, 2003.
[113] F. Tröltzsch, *Optimal control of partial differential equations: Theory, methods, and applications*, in: Graduate Studies in Mathematics, Vol. 112, AMS, 2010.
[114] C. Valentin, J.-M. d'Herbès, and J. Poesen, *Soil and water components of banded vegetation patterns*, Catena, 37:1–24, 1999.
[115] J. van Belzen, J. van de Koppel, M. L. Kirwan, D. van der Wal, P. M. Herman, V. Dakos, S. Kéfi, M. Scheffer, G. R. Guntenspergen, and T. J. Bouma, *Vegetation recovery in tidal marshes reveals critical slowing down under increased inundation*, Nat. Commun., 8:15811, 2017.
[116] W. H. van der Putten et al., *Plant-soil feedbacks: The past, the present and future challenges*, Journal of Ecology, 101:265–276, 2013.
[117] E. H. van Nes and M. Scheffer, *Slow recovery from perturbations as a generic indicator of a nearby*

catastrophic shift, Am. Nat., 169:738–747, 2007.
[118] J. von Hardenberg, E. Meron, M. Shachak, and Y. Zarmi, *Diversity of vegetation patterns and desertification*, Phys. Rev. Lett., 87:198101, 2001.
[119] C. Wang, H. Wang, and S. Yuan, *Precipitation governing vegetation patterns in an arid or semi-arid environment*, J. Math. Biol., 87:22, 2023.
[120] X. Wang, J. Shi, and G. Zhang, *Bifurcation and pattern formation in an activator-inhibitor model with non-local dispersal*, Bull. Math. Biol., 84:140, 2022.
[121] E. Weerman, J. Van Belzen, M. Rietkerk, S. Temmerman, S. Kéfi, P. Herman, and J. Van de Koppel, *Changes in diatom patch-size distribution and degradation in a spatially self-organized intertidal mudflat ecosystem*, Ecology, 93:608–618, 2012.
[122] D. Wu, X. Zhao, S. Liang, T. Zhou, K. Huang, B. Tang, and W. Zhao, *Time-lag effects of global vegetation responses to climate change*, Glob. Change Biol., 21:3520–3531, 2015.
[123] Q. Xue, C. Liu, L. Li, G.-Q. Sun, and Z. Wang, *Interactions of diffusion and nonlocal delay give rise to vegetation patterns in semi-arid environments*, Appl. Math. Comput., 399:126038, 2021.
[124] Z.-C. Xue, J. Li, C.-H. Wang, G.-Q. Sun, and L. Li, *Multistability shifts in an aird vegetation system with nonlocal water absorption effect*, J. Math. Biol., 91:17, 2025.
[125] L. Yang, Q. Guan, J. Lin, J. Tian, Z. Tan, and H. Li, *Evolution of NDVI secular trends and responses to climate change: A perspective from nonlinearity and nonstationarity characteristics*, Remote Sens. Environ., 254:112247, 2021.
[126] Y. Yang, K. R. Foster, K. Z. Coyte, and A. Li, *Time delays modulate the stability of complex ecosystems*, Nat. Ecol. Evol., 7:1610–1619, 2023.
[127] Y. R. Zelnik, P. Gandhi, E. Knobloch, and E. Meron, *Implications of tristability in pattern-forming ecosystems*, Chaos, 28:033609, 2018.
[128] Y. R. Zelnik, S. Kinast, H. Yizhaq, G. Bel, and E. Meron, *Regime shifts in models of dryland vegetation*, Philos. Trans. Roy. Soc. A, 371:20120358, 2013.
[129] Y. R. Zelnik, Y. Mau, M. Shachak, and E. Meron, *High-integrity human intervention in ecosystems: Tracking self-organization modes*, PLoS Comput. Biol., 17:e1009427, 2021.
[130] Y. R. Zelnik, E. Meron, and G. Bel, *Gradual regime shifts in fairy circles*, Proc. Natl. Acad. Sci. USA, 112:12327–12331, 2015.
[131] H.-T. Zhang, Y.-P. Wu, G.-Q. Sun, C. Liu, and G.-L. Feng, *Bifurcation analysis of a spatial vegetation model*, Appl. Math. Comput., 434:127459, 2022.
[132] L.-X. Zhao, C. Xu, Z.-M. Ge, J. Van De Koppel, and Q.-X. Liu, *The shaping role of self-organization: Linking vegetation patterning, plant traits and ecosystem functioning*, Proc. R. Soc. B: Biol. Sci., 286:20182859, 2019.
[133] Q. Zhu et al., *An early warning signal for grassland degradation on the Qinghai-Tibetan Plateau*, Nat. Commun., 14:6406, 2023.